




# Presence of a [3Fe–4S] cluster in a PsaC variant as a functional component of the photosystem I electron transfer chain in *Synechococcus* sp. PCC 7002

Adam A. Pérez<sup>1,4</sup>  · Bryan H. Ferlez<sup>1,5</sup> · Amanda M. Applegate<sup>2,6</sup> · Karim Walters<sup>1</sup> · Zhihui He<sup>1</sup> · Gaozhong Shen<sup>1</sup> · John H. Golbeck<sup>1,2</sup>  · Donald A. Bryant<sup>1,3</sup> 

Received: 29 June 2017 / Accepted: 23 August 2017 / Published online: 15 September 2017  
© Springer Science+Business Media B.V. 2017

**Abstract** A site-directed C14G mutation was introduced into the stromal PsaC subunit of *Synechococcus* sp. strain PCC 7002 in vivo in order to introduce an exchangeable coordination site into the terminal F<sub>B</sub> [4Fe–4S] cluster of Photosystem I (PSI). Using an engineered PSI-less strain (*psaAB* deletion), *psaC* was deleted and replaced with recombinant versions controlled by a strong promoter, and the *psaAB* deletion was complemented. Modified PSI accumulated at lower levels in this strain and supported slower photoautotrophic growth than wild type. As-isolated PSI complexes containing PsaC<sub>C14G</sub> showed resonances with *g* values of 2.038 and 2.007 characteristic of a [3Fe–4S]<sup>1+</sup>

cluster. When the PSI complexes were illuminated at 15 K, these resonances partially disappeared and two new sets of resonances appeared. The majority set had *g* values of 2.05, 1.95, and 1.85, characteristic of F<sub>A</sub><sup>-</sup>, and the minority set had *g* values of 2.11, 1.90, and 1.88 from F<sub>B</sub>' in the modified site. The *S* = 1/2 spin state of the latter implied the presence of a thiolate as the terminal ligand. The [3Fe–4S] clusters could be partially reconstituted with iron, producing a larger population of [4Fe–4S] clusters. Rates of flavodoxin reduction were identical in PSI complexes isolated from wild type and the PsaC<sub>C14G</sub> variant strain; this implied equivalent capacity for forward electron transfer in PSI complexes that contained [3Fe–4S] and [4Fe–4S] clusters. The development of this cyanobacterial strain is a first step toward translation of in vitro PSI-based biosolar molecular wire systems in vivo and provides new insights into the formation of Fe/S clusters.

**Electronic supplementary material** The online version of this article (doi:10.1007/s11120-017-0437-0) contains supplementary material, which is available to authorized users.

✉ John H. Golbeck  
jhg5@psu.edu

✉ Donald A. Bryant  
dab14@psu.edu

<sup>1</sup> Department of Biochemistry and Molecular Biology, The Pennsylvania State University, University Park, PA, USA

<sup>2</sup> Department of Chemistry, The Pennsylvania State University, University Park, PA, USA

<sup>3</sup> Department of Chemistry and Biochemistry, Montana State University, Bozeman, MT, USA

<sup>4</sup> Present Address: Department of Pharmacology and Toxicology, University of Louisville, Louisville, KY 40202, USA

<sup>5</sup> Present Address: Department of Energy Plant Research Laboratory, Michigan State University, East Lansing, MI 28824, USA

<sup>6</sup> Present Address: Musculoskeletal Transplant Foundation, Jessup, PA 18434, USA

**Keywords** Cyanobacteria · Photosynthesis · Photosystem I · Iron–sulfur cluster · PsaC · Electron transfer

## Introduction

Cyanobacteria are unique photoautotrophic microorganisms that have recently gained prominence in the field of synthetic biology as platforms for producing commodity chemicals ranging from terpenes to biofuels (Ducat et al. 2011; Nozzi et al. 2013; Davies et al. 2014). Their advantages include faster growth rates and greater genetic tractability than their plant and algal counterparts (Ducat et al. 2011). Most importantly, cyanobacteria do not require arable land that could otherwise be used to grow food crops (Hellingwerf and Teixeira de Mattos 2009). Strategies to produce significant quantities of biofuels or commodities using cyanobacteria mainly

consist of metabolic flux engineering (Rupprecht et al. 2006; Angermayr et al. 2009; Hellingwerf and Teixeira de Mattos 2009; Savakis and Hellingwerf 2015). Products of the native pathways of CO<sub>2</sub> fixation and central carbohydrate metabolism are either redirected or enhanced to direct cellular resources into the production of a precursor molecule that can be further converted using heterologous enzymes (Machado and Atsumi 2012; Zhang et al. 2015).

An alternative approach to biofuel production uses the photosynthetic reaction center as a photochemical module to drive associated reactions based on redox chemistry (Lubner et al. 2010). Several solar biohydrogen systems have been devised that utilize Photosystem I (PSI) as the photosensitizer (Grimme et al. 2008; Iwuchukwu et al. 2010; Utschig et al. 2011, 2015; Silver et al. 2013). The approach of combining hydrogen-producing catalysts with PSI first generated interest when Greenbaum (1985) reported sustained hydrogen evolution by illumination of thylakoid membranes that had been treated with precipitated colloidal platinum. Lubner et al. (2011a, b) later demonstrated that directly tethering exogenous catalysts, e.g., hydrogenase, to the electron transfer chain of PSI via the terminal [4Fe–4S] cluster in the F<sub>B</sub> site of the stromal PsaC subunit in vitro is not only possible but could yield hydrogen production rates that exceed the rate of natural photosynthesis. Cyanobacterial PSI is a large multisubunit complex containing three [4Fe–4S] clusters, two phyloquinones, and six redox active chlorophyll *a* (Chl *a*) molecules (Jordan et al. 2001). PsaC is a ferredoxin-like subunit of PSI that harbors the two terminal [4Fe–4S] clusters designated F<sub>A</sub> and F<sub>B</sub> (Golbeck and Bryant 1991; Antonkine et al. 2002; Zhao et al. 1992; Jung et al. 1996; Jordan et al. 2001). PsaC has been the subject of extensive mutational studies to determine the identity of the cysteine ligands to the F<sub>A</sub> and F<sub>B</sub> clusters (Jung et al. 1997; Antonkine et al. 2002, 2009). It was during these efforts that substitution of the F<sub>B</sub> coordinating Cys 14 residue with Gly (C14G) was established as a basis for tethering exogenous components to PSI (Antonkine et al. 2007; Grimme et al. 2009).

In addition to providing the groundwork for tethering PSI to exogenous catalysts, mutational studies on PsaC provided much information pertaining to the properties and roles of Fe/S clusters in photosynthesis. Of particular relevance was the generation of cluster species not found naturally in PSI, including mixed-ligand [4Fe–4S] clusters and [3Fe–4S] clusters (Yu et al. 1995b). Mutations of the Cys residues coordinating the [4Fe–4S] clusters in PsaC generated variants containing a population of [3Fe–4S] clusters when the apoprotein was reconstituted in vitro (Zhao et al. 1992; Yu et al. 1993). Correct folding of holo-PsaC apparently requires at least one cubane [4Fe–4S] cluster in either the F<sub>A</sub> or F<sub>B</sub> site; no PsaC variant harboring two [3Fe–4S] clusters was ever obtained (Mehari et al. 1995). Furthermore,

reassembled P<sub>700</sub>–F<sub>X</sub> cores never included a PsaC variant with a [3Fe–4S] cluster even when such clusters were present in the unbound state. Instead, the reassembled PSI complexes contained one ‘normal’ cubane [4Fe–4S] cluster with four Cys ligands at the unmodified site and one mixed-ligand [4Fe–4S] cluster with three Cys and either one sulfur from 2-mercaptoethanol when Ala or Gly is substituted for the fourth Cys or one oxygen when Ser or Asp is substituted for the fourth Cys at the modified site (Yu et al. 1995b). This led to the long-standing conclusions that cubane [4Fe–4S] clusters are required for the correct folding of PsaC, for the assembly of PsaC into PSI complexes, and for the ability of PsaC to participate in the electron transfer chain from P<sub>700</sub> to F<sub>B</sub>. One important result from this work was the finding that an external thiol ‘rescue’ ligand to the modified F<sub>B</sub> cluster of PsaC results in a [4Fe–4S] cluster in a  $S = 1/2$  ground state, whereas an external oxygen ‘rescue’ ligand results in a [4Fe–4S] cluster in a  $S \geq 3/2$  spin state (Golbeck 1999). In the present study we demonstrate that PsaC harboring a  $S = 1/2$  mixed-ligand [4Fe–4S] cluster or a  $S = 1/2$  [3Fe–4S] cluster in the F<sub>B</sub> site can be stably bound to PSI in vivo and that both clusters appear to be capable of equivalent rates of electron transfer to external electron acceptors such as flavodoxin in vitro.

## Materials and methods

### Strains and culture conditions

*Synechococcus* sp. strain PCC 7002 (hereafter *Synechococcus* 7002) was obtained from the Pasteur Culture Collection (Institut Pasteur, Paris, France) (Rippka et al. 1979). Photoautotrophic strains of *Synechococcus* 7002 were grown in medium A<sup>+</sup> (Stevens and Porter 1980; Ludwig and Bryant 2011). Unless specified, cells were grown under “standard conditions,” as previously described, which are defined as 38 °C, 250 μmol photons m<sup>-2</sup> s<sup>-1</sup> white light, and sparging with 1% (vol/vol) CO<sub>2</sub> in air (Ludwig and Bryant 2011). A PSI-less strain (described below) was grown in medium A<sup>+</sup> supplemented with 20 mM glycerol and low irradiance (~10 μmol photons m<sup>-2</sup> s<sup>-1</sup>) (Shen and Bryant 1995; Zhang et al. 2014). Growth rates were measured as described previously (Pérez et al. 2016a). Antibiotics were supplied at the following concentrations when required: 20 μg gentamicin ml<sup>-1</sup>; 50 μg spectinomycin ml<sup>-1</sup>; and 100 μg kanamycin ml<sup>-1</sup>.

### Transformation procedure, PCR amplification, restriction enzyme digestions, and ligations

*Synechococcus* 7002 was transformed as described (Xu et al. 2011). Plasmids and strains developed and used in this study

are summarized in Table 1. Oligonucleotide primers utilized for genetic manipulations and screening of *Synechococcus* 7002 mutants in this study are provided in Table S1. The procedures employed for PCR amplifications, restriction enzyme digestions, and ligations are explained in detail in the Supplemental Materials.

**Generation of a *psaC* deletion strain and PsaC complemented strains**

*Synechococcus* 7002 strain GS001, a PSI-less strain with the *psaAB* locus partially replaced with the *aadA* spectinomycin cassette ( $\Delta ps a A B :: a a d A$ ) (Fig. 1a), has been described previously (Shen and Bryant 1995; Zhang et al. 2014). The chromosomal copy of *psaC* in the GS001 strain was replaced with the *aacC1* gene, which confers gentamicin resistance (Fig. S1). The resulting *psaAB psaC* mutant was designated as strain AAP100. The pAQ3Ex endogenous plasmid-based expression system (Xu et al. 2011) was used for *trans*-complementation of  $\Delta ps a C :: a a c C 1$  in strain AAP100 with the wild-type *psaC* gene and various site-specific mutations of *psaC* (Table 1; Fig. 2). Details of the construction of these strains can be found in the Supplemental Materials.

**Electrophoresis and immunoblot analysis**

Polyacrylamide gel electrophoresis (PAGE) with sodium dodecyl sulfate (SDS) was performed on 15% (wt/vol.) polyacrylamide gels (30.0:0.8 acrylamide/bisacrylamide) as described (Shen and Bryant 1995). Equal amounts of cells (100  $\mu$ l of  $OD_{730} = 4$ ) were centrifuged, and the cell pellets were resuspended in BugBuster™ protein extraction reagent (40  $\mu$ l) (Novagen, Madison, WI) (Zhang et al. 2014). Immunoblotting and detection was performed as described (Shen et al. 2002b). Polyclonal rabbit antibodies to the PsaC protein from *Synechococcus* 7002 were used (Yu et al. 2003).

**Low-temperature fluorescence spectroscopy (77K)**

Fluorescence emission spectra were measured as described (Shen and Bryant 1995; Zhang et al. 2014) using an SLM-Aminco 8100C spectrofluorometer modernized for computerized data acquisition by On-Line Instrument Systems (Bogart, GA). Cells were harvested in the exponential growth phase ( $OD_{730} \sim 0.7$ ) and resuspended in a solution of 50 mM Tris-HCl, pH 8.0 with 60% (vol/vol) glycerol. The cell density was adjusted to  $OD_{730} = 0.5$ , and the

**Table 1** Bacterial strains and plasmids used in this study

Plasmid/strain	Relevant characteristics	Source
<b>Plasmids</b>		
pAQ3Ex	pGEM-7zf pMB1 vector backbone with <i>Synechococcus</i> sp. strain PCC 7002 pAQ3 flanking sites, Km <sup>R</sup>	
pAQ3Ex- <i>P</i> <sub>cpcBA6803</sub> [ <i>psaC</i> <sub>WT</sub> ]	Expression of PsaC <sub>WT</sub> using <i>P</i> <sub>cpcBA6803</sub> , Km <sup>R</sup>	This study
pAQ3Ex- <i>P</i> <sub>cpcBA6803</sub> [ <i>psaC</i> <sub>C14G/C34S</sub> ]	Expression of PsaC <sub>C14G/C34S</sub> using <i>P</i> <sub>cpcBA6803</sub> , Km <sup>R</sup>	This study
pAQ3Ex- <i>P</i> <sub>cpcBA6803</sub> [His <sub>10</sub> - <i>psaC</i> <sub>C14G/C34S</sub> ]	Expression of His <sub>10</sub> -PsaC <sub>C14S/C34S</sub> using <i>P</i> <sub>cpcBA6803</sub> , Km <sup>R</sup>	This study
pET-36C	pUC19-derived plasmid to express <i>psaC</i> mutants under the T7 promoter, Ap <sup>R</sup> ; a pUC9-	
pAQEEmr80	Derived plasmid containing the <i>psaAB</i> locus and an inserted <i>ermC</i> cassette, Em <sup>R</sup>	
<b>Strains</b>		
<i>Synechococcus</i> sp. strain PCC 7002		Rippka et al. (1979)
<i>Escherichia coli</i> TOP10F'	F' { <i>lacIq</i> , <i>Tn10</i> ( <i>Tet</i> <sup>R</sup> )} <i>mcrA</i> $\Delta$ ( <i>mrr</i> - <i>hsdRMS</i> - <i>mcrBC</i> ) $\Phi$ 80 <i>lacZ</i> $\Delta$ <i>M15</i> $\Delta$ <i>lacX74</i> <i>recA1</i> <i>araD139</i> $\Delta$ ( <i>ara leu</i> ) 7697 <i>galU</i> <i>galK</i> <i>rpsL</i> ( <i>Str</i> <sup>R</sup> ) <i>endA1 nupG</i>	Invitrogen
<b>Constructed strains</b>		
GS001	$\Delta ps a A B :: a a d A$	
AAP100	$\Delta ps a A B :: a a d A ps a C :: a a c C 1$	This study
AAP101	pAQ3Ex- <i>P</i> <sub>cpcBA6803</sub> [ <i>psaC</i> <sub>WT</sub> ] $\Delta ps a A B :: a a d A ps a C :: a a c C 1$	This study
AAP102	pAQ3Ex- <i>P</i> <sub>cpcBA6803</sub> [ <i>psaC</i> <sub>C14G/C34S</sub> ] $\Delta ps a A B :: a a d A ps a C :: a a c C 1$	This study
AAP103	pAQ3Ex- <i>P</i> <sub>cpcBA6803</sub> [His <sub>10</sub> - <i>psaC</i> <sub>C14G/C34S</sub> ] $\Delta ps a A B :: a a d A ps a C :: a a c C 1$	This study
AAP104	pAQ3Ex- <i>P</i> <sub>cpcBA6803</sub> [ <i>psaC</i> <sub>WT</sub> ] pAQEEmr80 <i>psaC</i> :: <i>aacC1</i>	This study
AAP105	pAQ3Ex- <i>P</i> <sub>cpcBA6803</sub> [ <i>psaC</i> <sub>C14G/C34S</sub> ] pAQEEmr80 <i>psaC</i> :: <i>aacC1</i>	This study
AAP106	pAQ3Ex- <i>P</i> <sub>cpcBA6803</sub> [His <sub>10</sub> - <i>psaC</i> <sub>C14G/C34S</sub> ] pAQEEmr80 <i>psaC</i> :: <i>aacC1</i>	This study

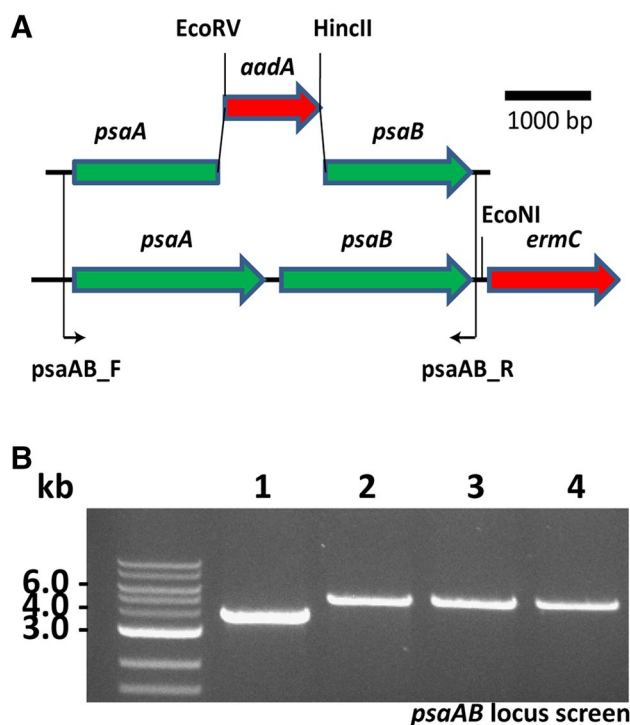


**Fig. 1** Complementation of a partial deletion of *psaAB* with plasmid pAQEEmr80. **a** Diagram showing the complementation of the partial *psaAB* deletion mutant, in which a portion of the *psaA* and *psaB* genes had been replaced by an *aadA* cassette, in strains AAP101, AAP102, and AAP103. Transformants were selected by their photoautotrophic phenotype. The positions of primers to screen allele segregation are illustrated. Primer sequences are available in Table S1. **b** Results of agarose gel electrophoresis of amplicons produced by screening primers *psaAB\_F* and *psaAB\_R* showing full segregation of the *psaAB* and  $\Delta$ *psaAB::aadA* alleles. Colony PCR templates from *Synechococcus* sp. strain PCC 7002 strains AAP100 (lane 1), wild type (lane 2), AAP104 (lane 3), and AAP106 (lane 4) were used

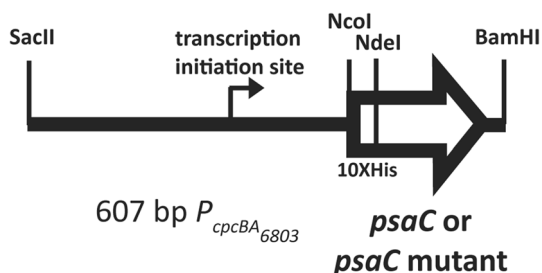


**Fig. 2** Diagram representing the organization of genetic elements for expression of *psaC* genes in the pAQ3Ex expression platform. The *psaC* genes were expressed using the strong constitutive  $P_{cpcBA(6803)}$  promoter (Zhou et al. 2014). Proteins can be produced with and without a poly-His affinity tag using the unique *SacII* and *NcoI* or the *SacII* and *NdeI* restriction sites, respectively

samples were frozen in liquid nitrogen for data acquisition of Chl *a* fluorescence emission using 440 nm as the excitation wavelength.

## Pigment analysis

Chl *a*, carotenoid, and phycobiliprotein concentrations were measured as described previously (Sakamoto and Bryant 1998; Zhang et al. 2014). Pigment concentrations were compared on the basis of equal cell numbers as described previously (Sakamoto and Bryant 1998).

## Total mRNA profiling

Transcriptome profiling was performed as described previously (Ludwig and Bryant 2011; Pérez et al. 2016b). rRNA was removed from total RNA using the Ribo-Zero™ rRNA Removal Kit for bacteria (Epicentre, Madison, WI), and cDNA library construction and Illumina sequencing was performed in the Genomics Core Facility at The Pennsylvania State University, University Park, PA (Gan et al. 2014; Zhang et al. 2014). The RNA sequencing data were deposited in the NCBI Sequence Read Archive (SRA) under Accession Number SRP087652.

## EPR spectroscopy

Continuous-wave (CW) electron paramagnetic resonance (EPR) spectroscopic measurements were carried out using a Bruker E500 spectrometer at X-Band (9 GHz) with a cylindrical TE 011 mode resonator (Bruker BioSpin Corp). The temperature was maintained at 15 K using a liquid helium ESR-910 cryostat and ITC-4 controller (Oxford Instruments). Illumination of the sample in the resonator was provided using a continuous-wave laser at 532 nm (Verdi-V5, Coherent) passing through a 3× beam expander (Oriel). Data represent the average of 16 scans. Trimeric fractions of PSI from wild-type and mutant strains of *Synechococcus* 7002 were purified as described previously except that *n*-dodecyl β-D-maltoside (DDM) was used instead of Triton X-100 (Schluchter et al. 1996). PSI samples (200 μl) were prepared with a final concentration of either 0.5 or 2 mg Chl *a* ml<sup>-1</sup> in 50 mM Tris-HCl pH 8.0, 10 mM MgCl<sub>2</sub>, 5 mM CaCl<sub>2</sub>, 0.05% (vol/vol) DDM, 20% (vol/vol) glycerol, 10 mM Na-ascorbate, and 10 μM 1,6-dichlorophenolindophenol (DCPIP). Cyanobacterial cells for EPR analysis were standardized to a sample volume of 200 μl with an OD<sub>730</sub> = 80 under the same buffer conditions and with the same electron donors as for the purified PSI complexes. Samples were frozen in darkness and illuminated inside the EPR cavity to promote one electron to either F<sub>A</sub> or F<sub>B</sub>. Alternatively, samples were illuminated continuously while freezing (295–15 K) to allow for multiple turnovers that allow one to observe interaction spectra with electrons residing on both F<sub>A</sub> and F<sub>B</sub> (Vassiliev et al. 2001). For chemical reduction experiments, purified PSI complexes were treated with excess sodium dithionite in 0.1 M glycine, pH 10.0. The

presence of high-spin clusters and the reduced state of a  $[3\text{Fe-4S}]^0$  cluster were assessed by recording spectra at 4 K as described previously (Yu et al. 1995b, c). Reconstitution of the iron–sulfur clusters of the  $\text{PsaC}_{\text{C14G/C34S}}$ -PSI complex from strain AAP106 was based on a protocol previously developed for apo-PsaC (Jung et al. 1995).

### Time-resolved optical spectroscopy

Time-resolved optical kinetics of charge recombination in detergent-solubilized PSI samples were measured using a commercial JTS-10 pump–probe spectrometer (BioLogic LLC). The probe light was selected by placing an interference filter (FWHM = 10 nm, Edmund Optics) in front of the stock 810 nm LED diode module. Excitation light was provided by a Clark MXR ORC-1000 Nd:YAG laser with a pulse width of ~400 ns and single pulse energy of 2 mJ at 532 nm. Data represent the average of three light-minus-dark excitation events. The sample that was exposed to the pulsed 532-nm excitation source was subtracted from a ‘dark’ trace, for which the pulsed laser was fired but physically blocked from hitting the sample to remove an electrical artifact. Samples were composed of PSI at a concentration of 50  $\mu\text{g Chl } a \text{ ml}^{-1}$  in 50 mM Tris–HCl pH 8.0, 10 mM  $\text{MgCl}_2$ , 5 mM  $\text{CaCl}_2$ , 10  $\mu\text{M}$  DCPIP, 10 mM sodium ascorbate, and 0.05% (vol/vol) DDM.

### Flavodoxin photoreduction assay

Rates of flavodoxin photoreduction were measured as described previously (Xu et al. 1994). The rate of change in absorption of flavodoxin was measured at 467 nm (Zhao et al. 1998) using a Cary 219 spectrophotometer as previously described (Xu et al. 1994). Samples were prepared utilizing 15  $\mu\text{M}$  flavodoxin (400  $\mu\text{l}$ ) and purified PSI complexes at 5  $\mu\text{g Chl } a \text{ ml}^{-1}$  in 50 mM Tris–HCl pH 8.0, 10 mM  $\text{MgCl}_2$ , 5 mM  $\text{CaCl}_2$ , and 0.05% (vol/vol) DDM. Electron donors in the reaction consisted of 10 mM Na-ascorbate and 10  $\mu\text{M}$  DCPIP.

## Results

### The *psaC* gene is essential for photoautotrophy in *Synechococcus* 7002

Repeated attempts to delete the *psaC* gene (SYNPCC7002\_A1589) from wild-type *Synechococcus* 7002 produced only merodiploid strains (Fig. S2). Strain GS001, a light-sensitive, photomixotrophic, PSI-less strain of *Synechococcus* 7002 with a partially deleted *psaAB* locus (Fig. 1a; Table 1) (Cantrell and Bryant 1987; Shen and Bryant 1995), was used as the background strain to delete the chromosomal

copy of *psaC* (Fig. S1a). Full segregation of the *psaC* and  $\Delta\text{psaC}::\text{aacCI}$  alleles was confirmed by PCR analysis (Fig. S1b) and DNA sequencing. The resulting strain, AAP100, was complemented in *trans* with various *PsaC* constructs (Fig. 2). To ensure that no unexpected changes occurred, all relevant gene sequences were confirmed both before and after complementation. Complementation of the  $\Delta\text{psaAB}::\text{aadA}$  locus (Fig. 1a) allowed for rescue of PSI complexes containing variant *PsaC* subunits, including the  $\text{PsaC}_{\text{C14G/C34S}}$  variant (hereafter, simply termed the  $\text{PsaC}_{\text{C14G}}$  variant, because Cys 34 is not a ligand to the iron–sulfur clusters, and the change to Ser simply reduces the chance of forming protein dimers and misfolding). The complemented *psaAB* locus in strains with genes encoding variant *PsaC* subunits was also verified by PCR (Fig. 1b) and by DNA sequencing. The results demonstrated that *psaC* is not an essential gene in *Synechococcus* 7002 mutant strains lacking PSI. Photoautotrophic transformants were never obtained when the  $\Delta\text{psaAB}::\text{aadA}$  locus in strain AAP100 was complemented with pAQEEmr80. These results demonstrate that the *psaC* gene product is essential for PSI activity, but PSI activity is not required for viability of *Synechococcus* 7002 under photoheterotrophic growth conditions (Shen and Bryant 1995; Zhang et al. 2014).

### *psaC* variants can be expressed in *trans* to rescue PSI activity

*PsaC* was not detected in strain AAP100 (Fig. 3a, lane 4) as expected, but production of *PsaC* was confirmed by immunoblotting in the complemented strains AAP104 and AAP106 (Fig. 3a, lanes 2 and 3). Because strains AAP104 and AAP106 were capable of photoautotrophic growth, they no longer required glycerol as a carbon source. Strain AAP100 did not exhibit any PSI-associated Chl *a* low-temperature (77K) fluorescence emission (Fig. 4b). However, strains AAP104 (Fig. 4c) and AAP106 (Fig. 4d) exhibited an emission peak from Chl *a* associated with PSI; moreover, the emission spectra observed were similar to those of the wild type (Fig. 4a). As judged by the amplitudes of the associated Chl *a* fluorescence emission, the Photosystem II (PSII):PSI ratio is higher in strain AAP106 than in strain AAP104 or the wild type (Fig. 4d).

### Pigment analysis and growth of strains complemented with *PsaC* variants

Strain AAP106 is bluer in color than the wild type and strain AAP104 of *Synechococcus* 7002 (Fig. 3b). Pigment analyses of these strains (Table 2) showed that strain AAP106 contains ~60% more phycobiliproteins and ~58% less Chl *a* than the wild type. The carotenoid contents for strains AAP104 and AAP106 were more similar, although strain

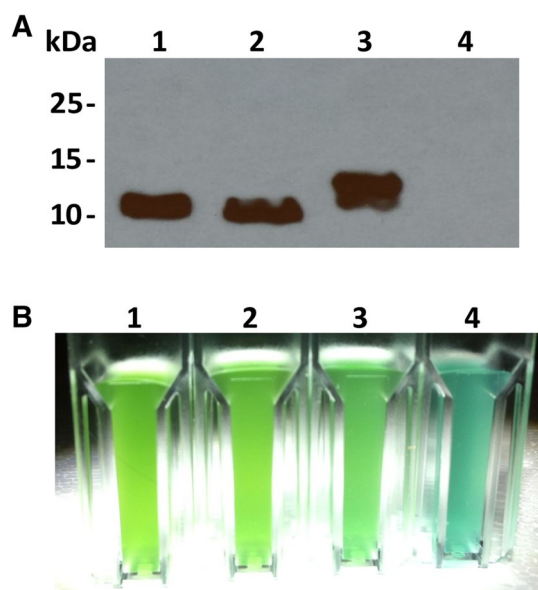


**Fig. 3** **a** Immunoblot analysis of PsaC in whole cells of strains complemented with variant *psaC* genes. Equal amounts of cells were used to produce the whole-cell extracts of wild-type (WT) *Synechococcus* 7002 (lane 1), and of strains AAP104 (lane 2), AAP106 (lane 3), and AAP100 (lane 4), which were used for immunoblot analysis with anti-PsaC<sub>7002</sub> antibodies. **b** Appearance of cultures of *Synechococcus* 7002 wild type (cuvette 1) and strains AAP104 (cuvette 2), AAP106 (cuvette 3), and AAP100 (cuvette 4)

AAP106 had 15% higher carotenoid content than the wild type. These results were similar regardless of whether the gene encoding [His]<sub>10</sub>-tagged (strain AAP106) or untagged PsaC<sub>C14G/C34S</sub> (strain AAP105) variant was used to complement the *psaC* deletion.

The Chl *a* and carotenoid contents of strain AAP100 were significantly lower than those of the wild type and AAP106. This is because strain AAP100 lacks PSI, which binds a large proportion of the Chl *a* and the carotenoids in cyanobacterial cells. The pigment content of strain AAP104 differed from that of the wild type and had a lower phycobiliprotein content than the PSI-less strain AAP100 (Table 2). The phycobiliprotein, Chl *a*, and carotenoid contents of strain AAP104 were 45%, ~68%, and 123% of the wild-type values, respectively.

Strains AAP104 and AAP106 grow photoautotrophically but have longer doubling times than wild type (Fig. 5). The calculated doubling times were  $4.51 \pm 0.14$  h for wild-type *Synechococcus* 7002,  $5.76 \pm 0.13$  h for strain AAP104, and  $8.78 \pm 0.10$  h for strain AAP106. The longer doubling times correlate well with the lower Chl *a* and PSI contents of strains AAP104 and AAP106 (Table 2; Fig. 5).

#### Extensive transcriptional changes in the PsaC<sub>C14G/C34S</sub> complemented strain

To understand the observed physiological differences, the transcriptome of strain AAP106 under standard growth

**Fig. 4** Low-temperature (77K) fluorescence emission spectra of whole cells of various strains of *Synechococcus* 7002. The excitation wavelength was 440 nm to preferentially excite Chl *a*. PSII indicates PSII and PSI indicates PSI. **a** The *Synechococcus* 7002 wild-type strain shows the ~720 nm Chl *a* emission maximum characteristic of PSI as well as maxima at 685 and 695 characteristic of PSII. **b** Strain AAP100 which lacks PSI; the characteristic PSI emission maximum at ~720 nm is absent, whereas the two emission peaks at 685 and 695 nm characteristic of PSII are present. **c** The emission spectrum for strain AAP104 shows emission maxima for both PSI and PSII and is similar to that of the wild-type strain. **d** The emission spectrum for strain AAP106 shows maxima characteristic of both PSI and PSII, albeit at a different ratio than the AAP104 and wild-type strains

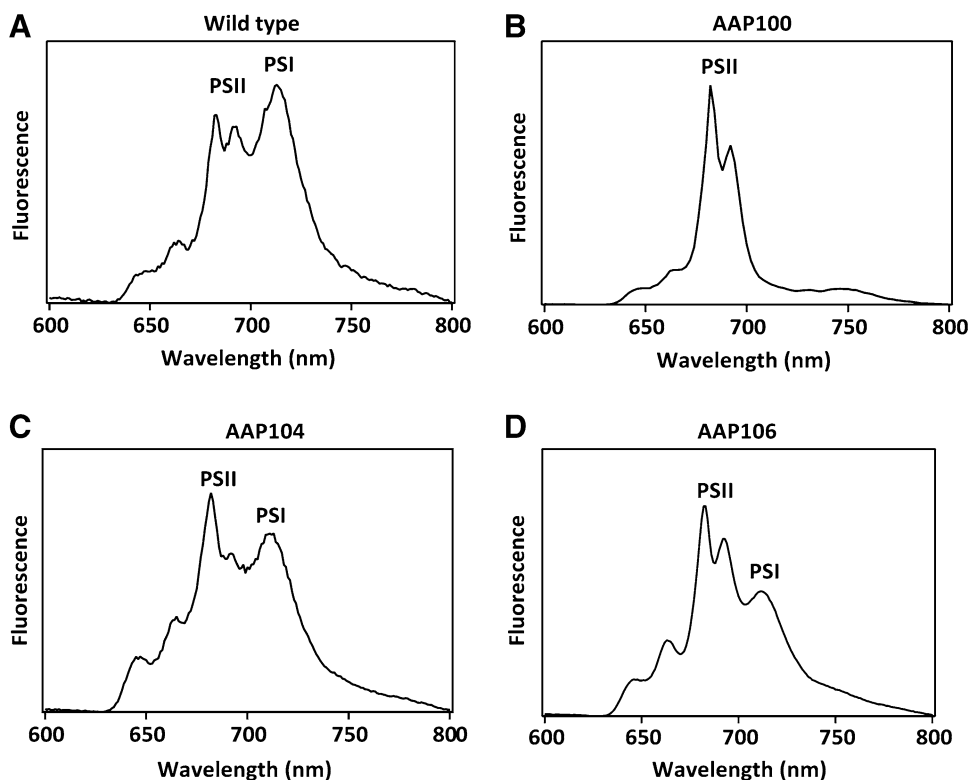


**Table 2** Pigment analysis of *Synechococcus* 7002 strains

	Chlorophyll <i>a</i> ( $\mu\text{g ml}^{-1} \text{OD}_{730}^{-1}$ )	Carotenoids ( $\mu\text{g ml}^{-1} \text{OD}_{730}^{-1}$ )	Phycobiliproteins (relative units)
Wild type	7.22 ± 0.39	2.29 ± 0.15	414 ± 29
AAP100 <sup>a</sup>	0.89 ± 0.04	0.16 ± 0.02	341 ± 30
AAP104	4.93 ± 0.39	3.00 ± 0.27	189 ± 11
AAP105	4.19 ± 0.37	3.30 ± 0.28	634 ± 16
AAP106	4.25 ± 0.39	2.72 ± 0.08	640 ± 11

<sup>a</sup>Grown photoheterotrophically (20 mM glycerol) at low irradiance ( $\sim 10 \mu\text{mol photons m}^{-2} \text{s}^{-1}$ )

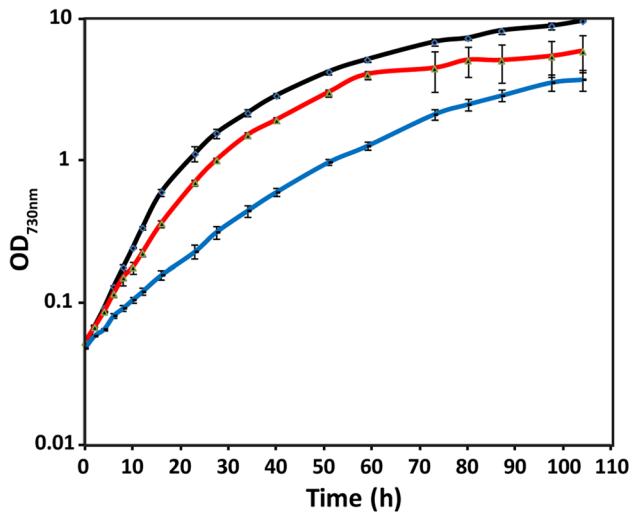


**Fig. 5** Comparison of the photoautotrophic growth behaviors for the wild type (black line) and strains AAP104 (red line) and AAP106 (blue line) of *Synechococcus* sp. PCC 7002. Growth was monitored for a period of 108 h. The data are the average of three parallel biological replicates for each strain, and the error bars represent the standard deviation

conditions was compared to that of the wild type. The relative transcript abundances of 295 genes increased by more than twofold in strain AAP106, while the relative transcript levels of 401 genes decreased by at least 50%. The complete RNAseq data can be found at the NCBI Sequence Read Archive (SRA) under accession number SRP087652. Figure 6 shows a scatter plot that compares the relative transcript abundances for all genes in strain AAP106 and wild type. Selected genes are identified in Fig. 6, and Table S2 provides a qualitative comparison of selected transcripts [a complete listing of transcript levels can also be found in (Pérez 2016)].

The relative transcript levels for the *sasA* adaptive-response sensory kinase, the *livF* ATP-binding protein for branched amino acid transport, and open reading frame SYNPC7002\_A2819 (glycosyl hydrolase family) increase >100-fold, when compared to the corresponding

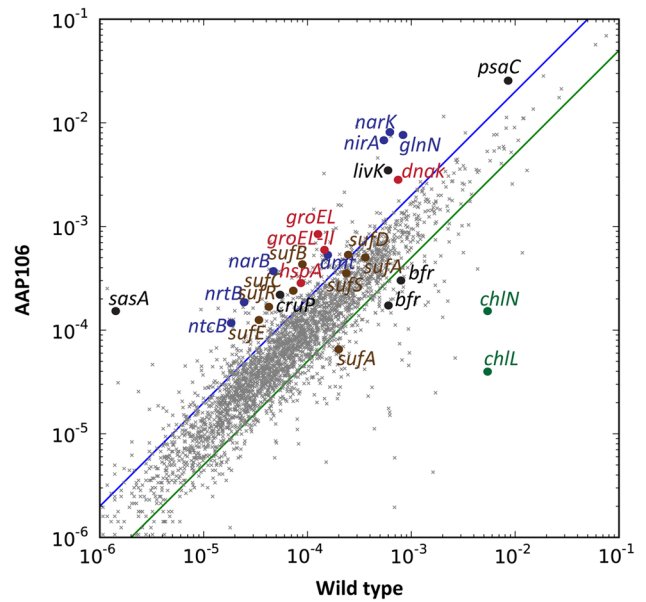


**Fig. 6** Scatter plot comparing the relative transcript abundances for mRNAs of strain AAP106 and wild-type strain of *Synechococcus* sp. strain PCC 7002. The blue line indicates a twofold increase in relative transcript abundance, while the green line indicates a 50% reduction in relative transcript level. The complete RNA sequencing data were deposited to the NCBI Sequence Read Archive (SRA) under Accession Number SRP087652

levels in wild-type *Synechococcus* 7002. Conversely, the *chlN* genes, encoding subunits of the light-independent protochlorophyllide reductase (Suzuki and Bauer 1992), showed the greatest decrease in transcript levels compared to wild type (136-fold lower for *chlL* and 34-fold lower for *chlN*; Table S2). Interestingly, the relative transcript levels for the *suf* regulon, which encodes genes related to iron-sulfur cluster biogenesis and regulation, increased significantly (Jin et al. 2008; Shen et al. 2007; Wang et al. 2004). The relative transcript levels for the *sufB*, *sufE*, *sufC*, *sufD*, and *sufR* genes on average increased at least twofold in strain AAP106 in comparison to wild-type *Synechococcus* 7002. Transcript levels decreased to 30% of the wild-type level for *sufA* (SYNPCC7002\_A2507). In general, relative transcript levels increased for genes encoding molecular chaperones in strain AAP106, including *groEL* (6.67-fold), *groEL-II* (4.11-fold), *groES* (3.64-fold), *dnaK* (3.65-fold), *hspA* (3.9-fold), and *htpG* (3.25-fold) (see Fig. 6 and Table S2). Transcript levels for numerous genes involved in nitrogen metabolism also increased in strain AAP106. For example, transcript levels for the nitrate transporter (*narK*) and for nitrite reductase (*nirA*) increased by 13-fold and 12-fold, respectively. The relative transcript levels for *narB*, *nrtB*, *ntcB*, *amt*, and *glnN* also increased by sixfold or more than the levels found in the wild type. Relative transcript levels for SYNPC7007\_A2663 and SYNPC\_A2664, encoding

two bacterioferritins, decreased to 28 and 37% of wild type, respectively, in strain AAP106. Compared to the wild type, the relative transcript levels for *isiA*, which encodes a Chl *a*-binding protein, and *isiB*, which encodes for flavodoxin, decreased by 74 and 83%, respectively. These changes suggest that, compared to the wild type, cells of strain AAP106 probably have excess available iron. The change in nitrogen-related genes might occur because of a limitation in reduced ferredoxin, which is required to reduce nitrate under the growth conditions employed.

Compared to wild type, the relative transcript levels of the genes of the sulfate ABC transporter (SYNPCC7002\_A0795-A0799) (Ludwig and Bryant 2012) were substantially lower in strain AAP106. Transcript levels for the *sbpA*, *cysT*, and *cysW* genes were 80, 74, and 54% lower, respectively, but transcript levels for SYNPCC7002\_A0799 and SYNPCC7002\_A0796, were similar to those of the wild type (Table S2). Transcript levels for genes required for sulfate reduction were unchanged or showed only a small decrease in strain AAP106. Transcripts for the *sat* gene, encoding sulfate adenosyltransferase (SYNPCC7002\_A1344), and *cysH* gene, encoding the 3'-phosphoadenosine-5'-phosphosulfate reductase, decreased by 51 and 20%, respectively (Table S2). Relative transcript levels for the adenylyl sulfate kinase *cysC* (SYNPCC7002\_A1494) and sulfite reductase (SYNPCC7002\_A2629) genes were similar in the two strains. Genes for enzymes required for biosynthesis of two endogenous thiol-containing compounds, cysteine and glutathione, which could potentially act as rescue ligands to the exchangeable coordination site of the  $F_B$  site in strain AAP106, showed mixed results. Relative transcript levels for *cysK* and *cysM*, encoding cysteine synthase, decreased slightly compared to the wild type (11 and 31%, respectively). However, relative transcript levels for *cysE*, encoding serine acetyltransferase, increased by 50% compared to wild type. The relative transcript level for *gshB*, encoding glutathione synthase, decreased by 29%, whereas the relative transcript level for the *gshA* gene, encoding glutamate–cysteine ligase, increased by 30% in strain AAP106.

Unexpectedly, the RNAseq data (Table S2) showed that the relative transcript levels for the genes encoding subunits of ATP synthase, with the exception of SYNPCC7002\_A0750 (*atpE*), increased modestly. Relative transcript levels for the *atpD*, *atpA*, *atpG*, *atpH*, *atpB*, and *atpF* genes were 1.3- to 1.84-fold higher in strain AAP106 than in wild-type *Synechococcus* 7002.

### PSI complexes containing $\text{PsaC}_{\text{C14G/C34S}}$ exhibit a dark EPR signal at $g = 2.038$ and $2.007$

Trimeric PSI complexes were isolated from the AAP104, AAP106, and wild-type strains. The low-temperature EPR spectra of these PSI complexes are shown in Fig. 7 prior to

photoreduction (dark spectra) and after illumination at low temperature and subtraction of the corresponding dark spectra (light minus dark). As-isolated PSI complexes from the wild type (Fig. 7IA) and strain AAP104 (Fig. 7IIA) measured in darkness showed only a minor derivative-shaped feature at  $g = 2.005$  characteristic of an organic radical. This resonance may be associated with a small population of  $\text{P}_{700}^+$  that may have been generated by exposure to light prior to dark adaptation (Shen et al. 2002a). In contrast, as-isolated PSI complexes from strain AAP106 (Fig. 7IIIA) measured in darkness showed a signal with axial symmetry and resonances at  $g = 2.038$  and  $2.007$  characteristic of a  $[\text{3Fe-4S}]^{1+}$  cluster (Asso et al. 1995). The presence of these resonances in whole cells (Fig. 8) indicates that the  $[\text{3Fe-4S}]$  cluster is not an artifact of isolation. Additionally, these resonances were not observed in PSI complexes purified from the wild type (Fig. 7IA) or strain AAP104 (Fig. 7IIA) or in intact cells of these strains (Fig. 8a).

The EPR spectra of PSI complexes from the wild type (Fig. 7IB) and strain AAP104 (Fig. 7IIB) after freezing in darkness and illumination at 15 K are similar and show the characteristic resonances of  $F_A^-$  at  $g = 2.05$ , 1.95, and 1.85 or  $F_B^-$  at  $g = 2.07$ , 1.93, and 1.88 after a single turnover (Malikin and Bearden 1971; Vassiliev et al. 2001). Using an identical protocol, PSI complexes from strain AAP106 showed a diminution of the resonances at  $g = 2.038$  and  $2.007$ , indicating reduction, albeit incomplete, of the  $[\text{3Fe-4S}]$  cluster. It should be kept in mind that the reduction of the  $F_A$  and  $F_B$  clusters in PSI is also not complete at low temperatures; only about 35% of the electrons reach the Fe/S clusters and the 65% that reach  $A_{1A}^-$  and subsequently recombine with  $\text{P}_{700}^+$  (van der Est 2001). The spectrum also showed resonances for  $F_A^-$  at  $g = 2.05$ , 1.95, and 1.85 (Fig. 7IIIB) and a very minor set of resonances at  $g = 2.11$ , 1.90, and 1.88. The latter are similar to those seen in mixed-ligand  $[\text{4Fe-4S}]$  clusters in C14A and C14G mutants of *PsaC* that contain an external rescue thiolate contributed by 2-mercaptoethanol (Golbeck 1999). We therefore attribute these resonances in strain AAP106 to a small population of mixed-ligand  $[\text{4Fe-4S}]$  clusters in the modified  $F_B$  site, which we term  $F_B'$ , which contains a thiolate, possibly glutathione or cysteine, as the external rescue ligand. No resonances were found downfield around  $g = 5.5$  (Yu et al. 1995b), which could be from the mixed-ligand  $[\text{4Fe-4S}]$  cluster in the  $S = 3/2$  ground state (data not shown). Additionally, the ratio of reduced  $F_A$  to  $F_B'$  is higher in PSI from strain AAP106 than from the wild type. Because the two clusters in *PsaC* are separated by  $\sim 12.3 \text{ \AA}$  (center to center) (Jordan et al. 2001) and are in equilibrium, this indicates that the redox potential of the mixed-ligand  $F_B'$  cluster in strain AAP106 is lower than the all-Cys-ligated  $F_B$  cluster in the wild type. The spin concentrations of the  $[\text{3Fe-4S}]$  cluster and the mixed-ligand  $[\text{4Fe-4S}]$  clusters were not estimated, as the simulations of their overlapping



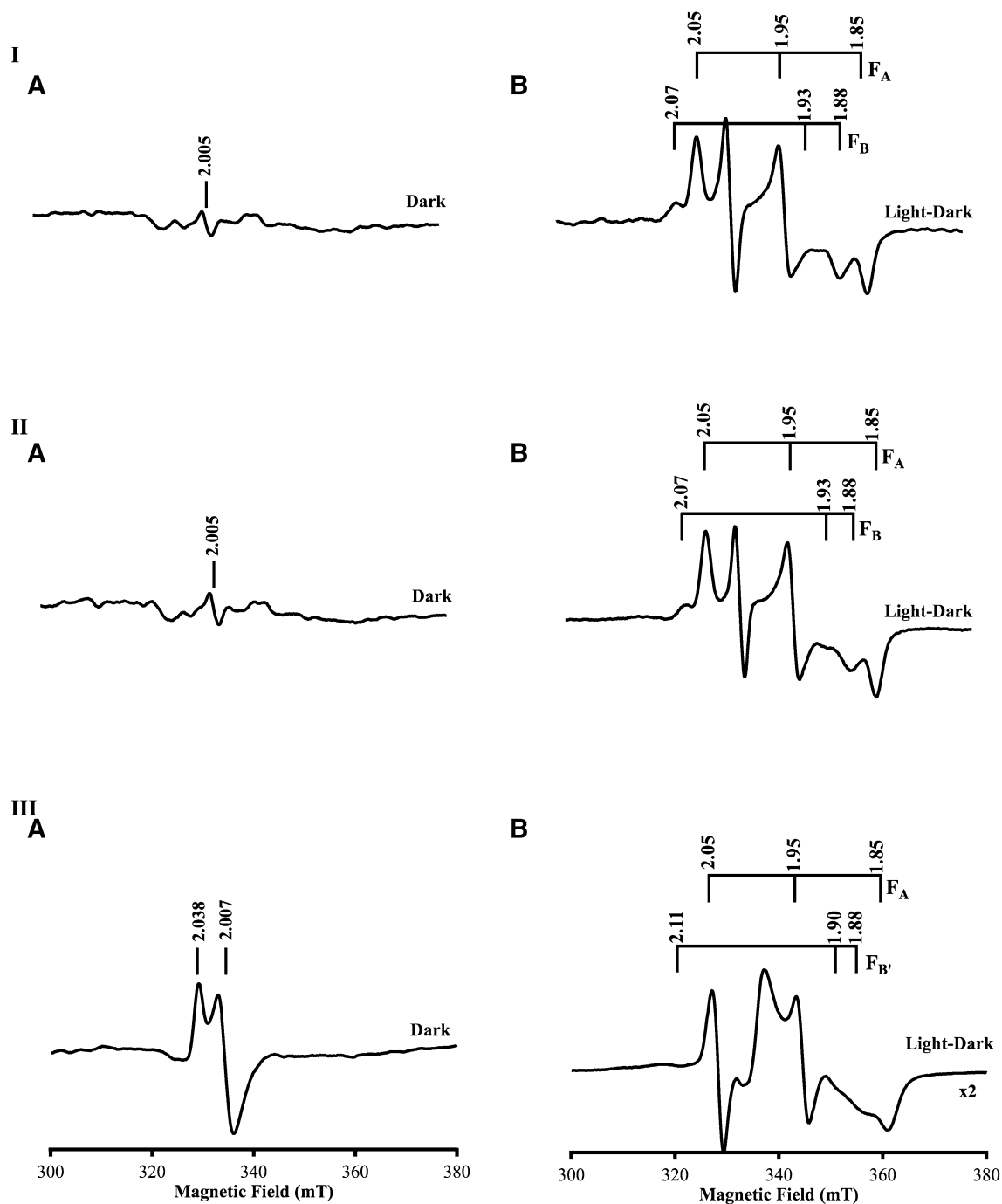


**Fig. 7** CW-EPR spectra of purified trimeric PSI complexes from *Synechococcus* sp. PCC 7002 strains complemented with variant *psaC* genes. Samples were frozen in darkness and illuminated after freezing at 15 K. Samples were adjusted to 0.5 mg Chl *a* ml<sup>-1</sup>. Spectra after illumination include the subtraction of the corresponding

dark spectrum. **I** Wild-type *Synechococcus* sp. strain PCC 7002 PSI trimers in the dark (*IA*) and after illumination (*IB*). **II** PSI trimers from strain AAP104 in the dark (*IIA*) and after illumination (*IIB*). **III** PSI trimers from strain AAP106 in the dark (*IIIA*) and after illumination (*IIIB*)

*g*-strained spectra (which also include the P<sub>700</sub><sup>+</sup> radical) resulted in unacceptable error.

Chemical reduction of the PSI samples with dithionite at pH 10.0 should result in reduction of the [3Fe–4S] cluster as shown by the loss of their resonances in the *g* = 2 region and

in the reduction of the normal and mixed-ligand [4Fe–4S] cluster(s). The EPR spectrum of PSI complexes from wild type and strain AAP104 (Figs. S3A, S3B) shows the so-called interaction spectrum of F<sub>A</sub><sup>-</sup>/F<sub>B</sub><sup>-</sup> with resonances at *g* = 2.05, 1.94, 1.92, and 1.88 (Malkin and Bearden 1971;

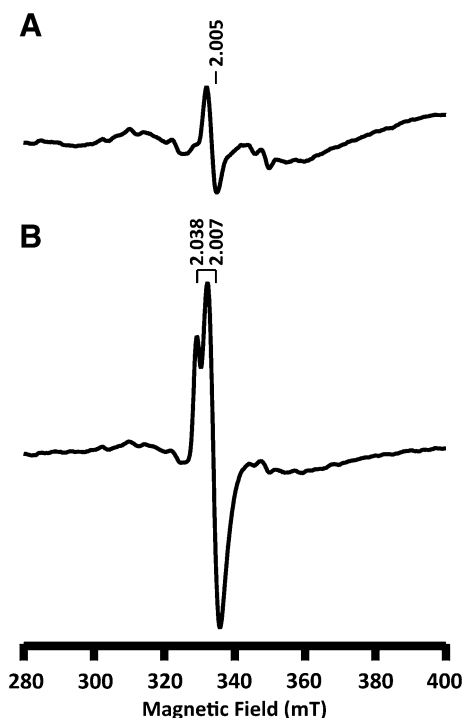


**Fig. 8** CW-EPR spectra of intact cyanobacterial cells. Intact cells (200  $\mu$ l) at an  $OD_{730\text{ nm}} = 80$  from wild-type *Synechococcus* sp. strain PCC 7002 (a) and strain AAP106 (b). Samples were frozen in the dark and spectra were collected at 15 K to test for the presence of a dark axial signal with resonances at  $g = 2.038$  and  $2.007$

Vassiliev et al. 2001), as well as a population of  $F_A^-$  only, which can be recognized by the unique feature at  $g = 1.85$  due to the presence of some non-reduced  $F_B$ . In contrast, the spectrum of PSI from strain AAP106 (Fig. S3C) shows primarily the resonances from  $F_A^-$  only at  $g = 2.05$ ,  $1.95$ , and  $1.85$ . The absence of an  $F_A^-/F_B^-$  interaction spectrum can be explained if the midpoint potential of  $F_B'$  in the mixed-ligand [4Fe–4S] cluster is sufficiently low that it cannot be reduced under the conditions that allow reduction of  $F_B$  in wild-type PSI.

An attempt was made to convert the [3Fe–4S] clusters to [4Fe–4S] clusters in isolated PSI complexes by addition of iron and inorganic iron–sulfur clusters. The latter are prepared from ferric chloride, sodium sulfide, and 2-mercaptoethanol, and consist of a mixed population of inorganic Fe, [2Fe–2S] and [4Fe–4S] clusters with thiol ligands provided by 2-mercaptoethanol (Golbeck 1995). After incubation, the signal with axial symmetry and resonances at  $g = 2.038$  and  $2.007$  was diminished, and the rhombic signal with  $g$  values of  $2.11$ ,  $1.90$ , and  $1.88$  was enhanced (Fig. 9), indicating partial reconstitution of the [3Fe–4S] clusters to mixed-ligand [4Fe–4S] clusters. The [3Fe–4S] clusters could not be completely reconstituted in spite of attempts that used high concentrations of iron and long incubation times. Nevertheless,

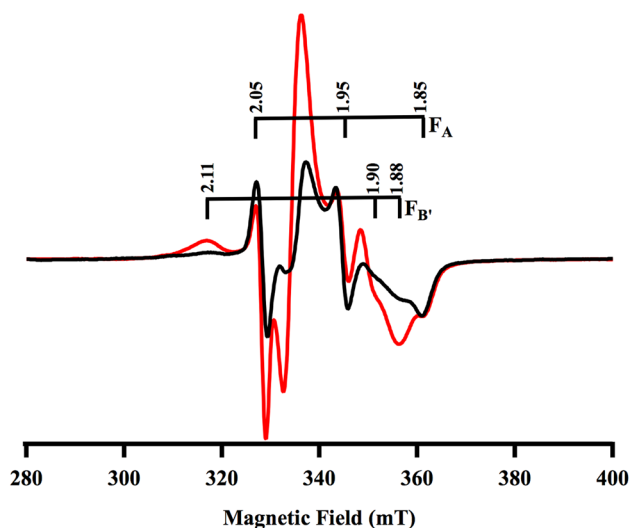


**Fig. 9** CW-EPR of reconstituted PSI trimers from strain AAP106 (see “Materials and methods”). Samples were frozen in darkness and illuminated after freezing at 15 K. The PSI trimer spectrum from AAP106 prior to reconstitution of Fe/S clusters (black line) was recorded at a Chl concentration of  $2\text{ mg Chl } a\text{ ml}^{-1}$ . The same sample was reconstituted in vitro (red line spectrum) and was at a concentration of  $1.24\text{ mg Chl } a\text{ ml}^{-1}$ . The difference in concentration required normalization of the spectra at the  $F_A^-$  resonance trough at  $g = 1.85$ . Each spectrum shown after illumination includes the subtraction of the corresponding dark spectrum. The characteristic  $g$  values for  $F_A^-$  are annotated for both spectra. The reconstituted sample (red line spectrum) generates enhanced  $F_B'$ -like resonances that are annotated as  $F_B'^-$

the conversion of [3Fe–4S] to [4Fe–4S] clusters supports their presence in the same modified  $F_B$  site (Fig. 9).

### Light-induced changes of $P_{700}$ in the near-IR

More accurate information about the stoichiometry of the [3Fe–4S] clusters and mixed-ligand [4Fe–4S] clusters in the modified  $F_B$  site can be obtained by time-resolved optical spectroscopy. While describing the data, it should be kept in mind that the charge recombination between  $[F_A/F_B]^-$  and  $P_{700}^+$  is not direct, but rather occurs by way of thermally activated, uphill electron transfer involving  $F_X$  and finally  $A_1^-$ , which then recombines with  $P_{700}^+$  (Shinkarev et al. 2002). The kinetics of charge recombination therefore depend on the difference in Gibbs free energy between each of the donor/acceptor pairs, as this specifies the equilibrium constant between the electron donor–acceptor pairs. If the modified cluster in the  $F_B$  site has a lower redox potential than the wild type,  $F_A$  will be more populated during the quasi-equilibrium process of recombination, and the rate of  $P_{700}^+$  reduction will appear faster; conversely, if the modified cluster in the  $F_B$  site has a higher redox potential than the wild type,  $F_A$  will be less populated during the

quasi-equilibrium process of recombination, and the rate of  $P_{700}^+$  reduction will appear slower.

To probe the charge recombination kinetics of PSI at room temperature, forward electron transfer from  $P_{700}$  to  $F_A/F_B$  was initiated using a saturating laser flash at 532 nm. The presence of  $P_{700}^+$  causes an immediate absorption increase at 820 nm, the amplitude of which is proportional

to its concentration. In the absence of an external electron acceptor, such as ferredoxin or flavodoxin, the charge recombination kinetics between  $P_{700}^+$  and  $[F_A/F_B]^-$  can be monitored by following the decrease in absorption at 820 nm as a function of time. The data (Table 3) show that the recombination kinetics of PSI complexes from the wild type and strain AAP104 exhibit a major decay phase with a lifetime of 84 ms (Fig. 10a) and 99 ms (Fig. 10b), respectively, which account for 77 and 79% of the total absorption change. This kinetic phase is derived from charge recombination between  $P_{700}^+$  and  $[F_A/F_B]^-$  (Vassiliev et al. 1997; Sauer et al. 1978). The remaining 21–23% of the total absorption change in PSI complexes derived from wild type and strain AAP104 is in the seconds time range (Fig. 10a, b) and can be attributed to electron transfer from exogenous donors to  $P_{700}^+$  in reaction centers that have lost the electron on  $F_B^-$  to molecular oxygen (Jung et al. 1996). The recombination kinetics of PSI complexes isolated from strain AAP106 (Fig. 10c) are considerably different (Table 3), and are characterized by four distinct kinetic phases. A 2-ms lifetime component, which accounts for 13.5% of the total absorption change, is typical of charge recombination between  $P_{700}^+$  and  $F_X^-$ . This indicates that a population of PSI cores is present that lack the PsaC, PsaD, and PsaE stromal subunits (Vassiliev et al.

**Table 3** Amplitudes of kinetic phases in time-resolved optical spectroscopy

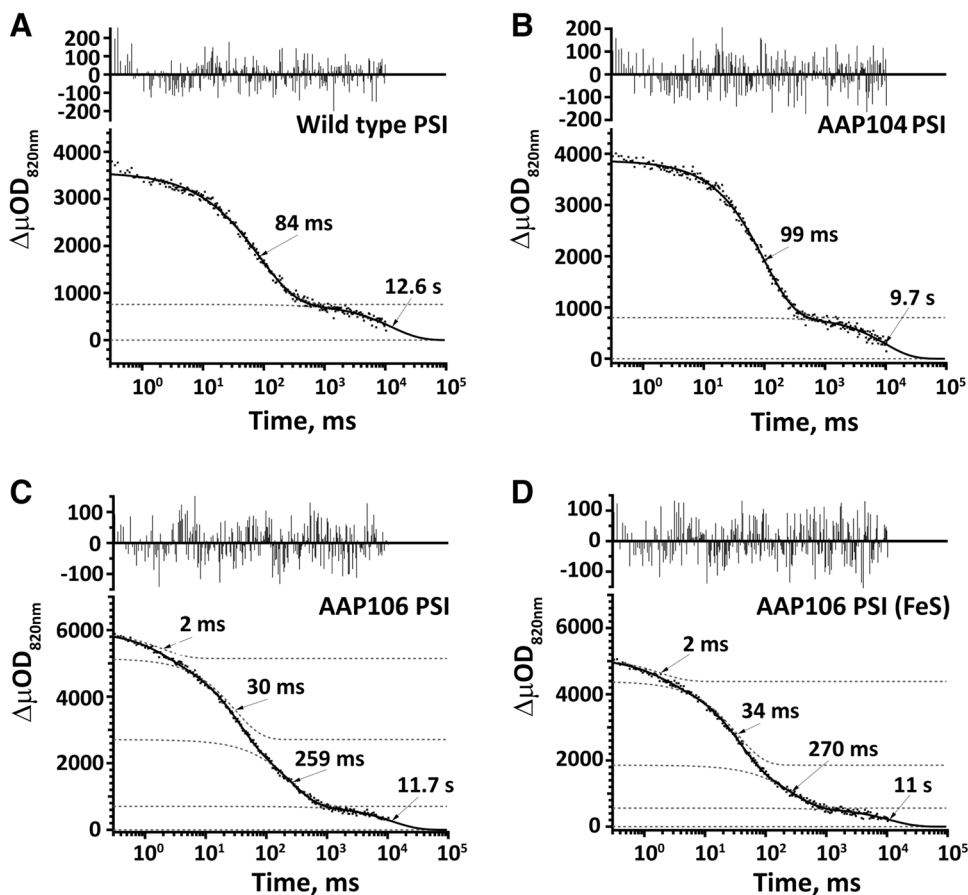
	Amplitude $\Delta\mu OD_{820nm}$			
	WT PSI	AAP104 PSI	AAP106 PSI	AAP106 PSI (FeS) <sup>a</sup>
$[F_A/F_B]^- \Rightarrow P_{700}^+$	77%	79%	N. P.	N. P.
DCPIP <sup>b</sup> $\Rightarrow P_{700}^+$	23%	21%	11.8%	12%
$F_X^- \Rightarrow P_{700}^+$	N. D. <sup>c</sup>	N. D.	13.5%	10%
$[F_A/F_B]^- \Rightarrow P_{700}^+$	N. P. <sup>c</sup>	N. P.	40.6%	54%
$[3Fe-4S]^0 \Rightarrow P_{700}^+$	N. P.	N. P.	34.1%	24%

<sup>a</sup>After in vitro FeS cluster reconstitution of AAP106 PSI particles

<sup>b</sup>DCPIP 1,6-dichlorophenolindophenol

<sup>c</sup>N. D. not detected; N. P. not present

**Fig. 10** Kinetics of flash-induced absorbance changes at 820 nm in PSI complexes containing variant PsaC proteins. Trimeric PSI complexes isolated from wild-type *Synechococcus* 7002 (a), strain AAP104 (b), strain AAP106 (c), and strain AAP106 after in vitro reconstitution of Fe/S clusters (d). For each sample, the lower portion of the panel presents the experimental points (dots) fitted by a multi-exponential decay (dotted lines). The solid line represents the sum of the multiple exponentials for each experiment. The upper panel represents the residual differences between the experimental data and fit curve (the solid line in lower panel)



1997; Sauer et al. 1978; Yu et al. 1995a). A 30-ms kinetic phase, which accounts for 40.6% of the total absorption change, is assigned to charge recombination between  $P_{700}^+$  and  $F_B^-$  in mixed-ligand [4Fe–4S] clusters that occupy the  $F_B$  site (Vassiliev et al. 2001). Its lifetime is nearly threefold faster than in wild-type PSI, which implies that the mixed-ligand [4Fe–4S] cluster has a lower redox potential than the all-Cys [4Fe–4S] cluster in wild-type PSI. A 259-ms kinetic phase, which is not observed in the wild type or AAP104-derived PSI complexes, is tentatively assigned to charge recombination from the [3Fe–4S]<sup>0</sup> cluster in the  $F_B$  site. Its lifetime is nearly threefold slower than  $F_B$  in wild-type PSI, which implies that the [3Fe–4S] cluster in the AAP106 variant has a higher redox potential than the all-Cys [4Fe–4S] cluster in wild-type PSI. It is noteworthy that the amplitudes of the 30- and 259-ms kinetic components are nearly equal, indicating equivalent subpopulations of PSI that contain either the [3Fe–4S] cluster or the mixed-ligand [4Fe–4S] cluster in the modified  $F_B$  site. Finally, a 11.7-s slow kinetic phase comprises 11.8% of the total absorption change and is attributed to electron transfer from exogenous donors to  $P_{700}^+$  in PSI complexes that have lost their electron from  $[F_A/F_B]^-$  (Jung et al. 1996). A significant fraction of this kinetic phase is probably derived from the population of PSI that contains the longer-lived [3Fe–4S] cluster rather than the shorter-lived [4Fe–4S] cluster due to the longer residence time of the electron on the former than the latter.

The recombination kinetics of reconstituted PSI derived from strain AAP106 (Fig. 10d) similarly contains four kinetic phases; however, the amplitude of the 34-ms phase is twice the amplitude of the 270-ms phase (Table 3). This change is in agreement with the EPR results, which show that some of the [3Fe–4S] clusters in the  $F_B$  site had been partially reconstituted to [4Fe–4S] clusters (see Fig. 8). These data further support the identification of the 30-ms and 259-ms kinetic phases from recombination with the [4Fe–4S] and [3Fe–4S] clusters, respectively, in the modified  $F_B$  site. It should be noted that when wild-type PsaC and a C14G variant of PsaC were combined with P700- $F_X$  cores in the presence of PsaD, the charge recombination times were 72.6 ms and 34.1 ms (Jung et al. 1996), values which are very similar to the 84-ms and 30-ms lifetimes reported in this work for the wild-type and the C14G/C34S variants of PsaC produced in vivo in *Synechococcus* 7002.

#### Forward electron transfer occurs with high efficiency in PSI with bound PsaC<sub>C14G</sub>

Purified PSI complexes from the wild type and strains AAP104 and AAP106, as well as strain AAP106 after iron–sulfur cluster reconstitution, were assayed for their ability to reduce flavodoxin when ascorbate and DCPIP were used as the electron donors (Fig. 11). The rates of flavodoxin

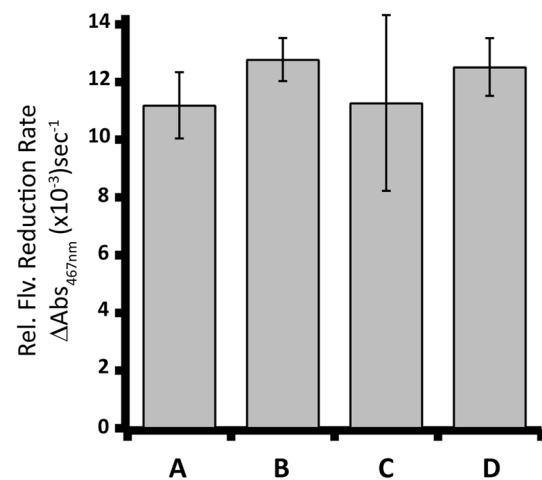


**Fig. 11** Flavodoxin reduction assay. Relative steady-state rates of flavodoxin reduction by PSI complexes isolated from wild-type *Synechococcus* 7002 (a); strain AAP104 (b); strain AAP106 (c); and strain AAP106 after in vitro reconstitution of Fe/S clusters (d). Each bar graph is the average of three independent measurements, and the error bars represent the standard deviation

reduction on a Chl basis for all of the PSI complexes with variant PsaC subunits, including the AAP106 strain, were statistically identical. Were the 50% population of PSI complexes containing [3Fe–4S] clusters in the  $F_B$  site unable to pass electrons forward to flavodoxin, the rate would have been expected to be one-half that of the wild type or the AAP104 strain. It thus appears that the [3Fe–4S] cluster can pass electrons forward to flavodoxin with the same efficiency as the all-Cys ligated [4Fe–4S]  $F_B$  cluster in wild-type PSI and the mixed-ligand [4Fe–4S]  $F_B'$  cluster in the modified site of AAP106.

## Discussion

### Incorporation of a C14G mutation in vivo in *Synechococcus* 7002

In this study, the C14G variant of PsaC was incorporated into PSI in *Synechococcus* 7002 as a first step towards employing molecular wire technology to tether redox enzymes in vivo. The idea was to eliminate the time-consuming task of removing the stromal subunits PsaC, PsaD, and PsaE from wild-type PSI and subsequently rebinding the stromal subunits with cloned and heterologously expressed and purified PsaD and a C14G variant of PsaC (Fig. 2) to generate a ligand exchangeable site on the terminal  $F_B$  cluster (Lubner et al. 2011a, b). Unlike earlier attempts in *Synechocystis* sp. strain PCC 6803 (hereafter *Synechocystis* 6803) (Yu et al. 1997), the resulting *Synechococcus* strain could grow photoautotrophically. Previous attempts in *Synechocystis* 6803 to

introduce PsaC variants in vivo were performed as knock-in substitutions into the *psaC* locus to allow transcription from the native promoter (Yu et al. 1997). When this strategy was attempted in *Synechococcus* 7002, the resulting strain was also unable to grow photoautotrophically (data not shown). It can be inferred that overexpression of apo-PsaC<sub>C14G</sub> increases the probability of introducing iron–sulfur clusters into PsaC—potentially as a [4Fe–4S] cluster with a labile iron atom or as a stable [3Fe–4S] cluster—into the F<sub>B</sub> site. Because of the different outcomes in these two organisms, we performed a thorough characterization of this mutant strain and its isolated PSI complexes.

### Characteristics of the [3Fe–4S] cluster and mixed-ligand [4Fe–4S] cluster in the modified F<sub>B</sub> site

Preliminary EPR studies of strain AAP106 showed that the characteristic resonances of the F<sub>B</sub> cluster with *g* values of 2.07, 1.93, and 1.88 (Zhao et al. 1992) in photoreduced, purified PSI complexes were missing (Fig. 7IIIB). Because these PSI complexes were still capable of forward electron transfer to flavodoxin, and because F<sub>A</sub> cannot transfer electrons directly to soluble ferredoxin/flavodoxin (Fischer et al. 1999), the data indicated that the F<sub>B</sub> site must be occupied by some type of iron–sulfur cluster. The low-temperature EPR spectrum of the as-isolated PSI complexes showed a dark signal with axial symmetry and resonances at *g* = 2.038 and 2.007 characteristic of a [3Fe–4S]<sup>1+</sup> cluster (Warren et al. 1993). These resonances were observed in intact cells as well as in isolated PSI complexes (Fig. 7IIIA and Fig. 8b), establishing that the [3Fe–4S] clusters were not artifacts of PSI isolation. We were not able to detect a low-field feature around *g* = 12 on reduction to the [3Fe–4S]<sup>0</sup> state, but as shown by previous studies on the [3Fe–4S] cluster-containing ferredoxin I (FdI) protein of *A. vinelandii* (Johnson et al. 1987), the absence of this feature should not be construed as evidence against its existence. The resonance may be absent simply because its zero-field splitting value is larger than the energy of the microwave photon at X-band. When the isolated PSI complexes from the AAP106 strain were illuminated at low temperature, the [3Fe–4S] clusters partly disappeared and two new resonances appeared at *g* = 2.05, 1.95, and 1.85 and at *g* = 2.11, 1.90, and 1.88. The former is due to the F<sub>A</sub> cluster in its unmodified site, and the latter is due to a mixed-ligand F<sub>B</sub>' cluster assigned to the modified site. The spin population of the mixed-ligand [4Fe–4S] cluster increases at the expense of the [3Fe–4S] cluster on addition of iron and iron–sulfur clusters. This correlates with the increase in amplitude of the 30 ms kinetic phase at the expense of the 259-ms kinetic phase on reconstitution with iron and iron–sulfur clusters.

In addition to the presence of a minor population of P<sub>700</sub>–F<sub>X</sub> cores, the data therefore indicate the presence of two subpopulations of PSI in the AAP106 strain. In one population, a mixed-ligand [4Fe–4S] cluster occupies the modified F<sub>B</sub> site, and in the second population a [3Fe–4S] cluster occupies the modified F<sub>B</sub> site. The mixed-ligand [4Fe–4S] F<sub>B</sub>' cluster has a lower midpoint potential than F<sub>B</sub> in the wild type as shown by the faster recombination time with P<sub>700</sub><sup>+</sup>. This conclusion is supported by the finding that sodium dithionite at pH 10 cannot reduce F<sub>B</sub>' in the modified site under conditions that reduce the majority of F<sub>B</sub> in wild-type PSI. The [3Fe–4S] cluster has a higher midpoint potential than F<sub>B</sub> in the wild-type PSI as shown by the slower recombination with P<sub>700</sub><sup>+</sup>. Indeed, a redox study of the similar C14A variant of unbound PsaC showed that the [3Fe–4S] cluster in the F<sub>B</sub> site has a midpoint potential of –171 mV, whereas the [4Fe–4S] cluster in the unmodified F<sub>A</sub> site has an unaltered midpoint potential of –551 mV (Mehari et al. 1995). Thus, in that population of PSI, which contains the mixed-ligand [4Fe–4S] cluster in the modified F<sub>B</sub> site, the equilibrium would tilt in favor of F<sub>A</sub> at the expense of F<sub>B</sub>', and very little reduced F<sub>B</sub>' would be observed by EPR. Conversely, in the population of PSI that contains the [3Fe–4S] cluster in the modified F<sub>B</sub> site, the equilibrium would tilt in favor of F<sub>B</sub> at the expense of F<sub>A</sub>, and very little reduced F<sub>A</sub> would be observed by EPR. The spectra shown in Fig. 7IIIB, 7IVB, and 8 reflect these trends in the superposition of spectra from these two respective populations of PSI.

### Identity of the rescue ligand in the modified F<sub>B</sub> site of PsaC

It is difficult to imagine the absence of a suitable ligand to the labile iron atom in the C14 position of PsaC<sub>C14G</sub>. We therefore assume that the corner iron in the modified F<sub>B</sub> site of the [4Fe–4S] cluster is bound by an external rescue ligand. Earlier work, which compared the spin state distributions of in vivo and in vitro C14 and C51 mutants of PsaC, showed that when an oxygen from Ser or Asp provided the rescue ligand, the mixed-ligand [4Fe–4S] cluster had a ground spin state of *S* = 3/2. Conversely, when the thiol from 2-mercaptoethanol provided the rescue ligand to the mixed-ligand [4Fe–4S] cluster in Ala or Gln mutants of PsaC, the ground spin state was *S* = 1/2 (Golbeck 1999). The finding of a *S* = 1/2 ground spin state in the [4Fe–4S] cluster in the modified F<sub>B</sub>' site of the C14G mutant implies that the external rescue ligand is a thiolate. One strong possibility is glutathione, which is present in millimolar concentrations in cyanobacteria (Cameron and Pakrasi 2010), or another small thiol-containing compound. This assumption is supported by the sulfate-replete intracellular conditions suggested from the downregulation of the sulfate ABC transporter operon (Table S2) (Ludwig and Bryant 2012)

in strain AAP106. Although genes for enzymes of sulfate reduction and glutathione biosynthesis did not change much in strain AAP106 compared to wild type, it is worth noting the increase in transcripts for genes encoding ATP synthase (Table S2). Some of the enzymes for sulfate reduction (Sat) and glutathione biosynthesis, notably GshA and GshB, are ATP-dependent (Anderson 1998). The possible increase in ATP synthase, combined with an apparent surplus of sulfate as suggested by the lower transcript levels for the sulfate transporter (Ludwig and Bryant 2012), could enhance glutathione biosynthesis and make this small thiol compound more readily available as a rescue ligand in strain AAP106.

Because the attempted reconstitution of the missing iron resulted in enhancement of the resonances at  $g = 2.12$ , 1.90, and 1.88, we can be confident that 2-mercaptoethanol accompanies the Fe in filling the empty site in the [3Fe–4S] cluster, thereby supporting the existence of a thiol group as the fourth ligand to the [4Fe–4S] cluster in vivo.

### Origin of the [3Fe–4S] cluster in the modified $F_B$ site of PsaC

While this may explain the presence of the [4Fe–4S] cluster in the modified  $F_B$  site, the question arises as to how the [3Fe–4S] cluster arises, especially since the evidence argues against it being an artifact of PSI isolation. Previous work from our laboratories showed that no PsaC variant that contained a [3Fe–4S] cluster could be rebound to PSI in vitro (Mehari et al. 1995). Incorporation of PsaC variants into PSI by site-specific mutagenesis of the analogous Cys ligand (C14) to  $F_B$  were first attempted in the cyanobacterium *Synechocystis* 6803, but none of the mutants generated were capable of photoautotrophic growth due to the very low amounts of PSI (Yu et al. 1997). It was concluded from those and related studies that PsaC requires two cubane [4Fe–4S] clusters for stable PSI complexes (Mehari et al. 1995). The issue therefore centers about how the ligand exchange reaction occurs in the hand-off of the assembled [4Fe–4S] cluster from a scaffold protein (like NfuA) to apo-PsaC (Jin et al. 2008; Roche et al. 2013). If, as is usually presumed, the Cys ligands of PsaC displace the ligands on the scaffold protein that temporarily carry the [4Fe–4S] cluster, the question is how the final Cys is displaced if there is a Gly in position 14 on PsaC. We propose that an endogenous thiolate such as glutathione displaces the fourth Cys residue of the scaffold protein, thereby completing the hand-off of the [4Fe–4S] cluster to the modified  $F_B$  site on PsaC. The rescue ligand is probably not protein-bound and hence it may either be labile or be displaced with a weaker ligand, which may be present in the cell at a higher concentration. In either event, its loss would likely lead to the loss of the iron atom, resulting in the [3Fe–4S] cluster in the modified  $F_B$  site.

These results imply that the ligand and Fe are lost from the labile site in the AAP106 variant after PsaC is bound. This process should be reversible, but we found it difficult to reinsert the iron atom into the missing site of the [3Fe–4S] cluster in the bound C14G PsaC mutant. One possibility is that the polypeptide backbone becomes exceptionally rigid in the presence of PsaD and PsaE, thereby inhibiting the insertion (as well as loss) of the Fe from the modified cluster. This would argue for the loss of the Fe during the assembly of the stromal subunits, and that after docking to form the stromal ridge, no further change occurs. It should be recalled that PsaE has not usually been used in in vitro reconstitution experiments (Golbeck 1995), and this may be an additional factor in conferring rigidity to PsaC.

### Forward electron transfer from the [3Fe–4S] and mixed-ligand [4Fe–4S] clusters to flavodoxin

Optical studies showed that strain AAP106 contains two approximately equal populations of PSI: one with a [3Fe–4S] cluster in the  $F_B$  site and the other with a mixed-ligand [4Fe–4S] cluster in the  $F_B$  site. On an equal Chl basis, this sample of PSI supports forward electron transfer to flavodoxin at rates that are identical to those of wild-type PSI (Fig. 11). This result might seem at variance with the slower growth rate of strain AAP106 compared to the wild type (Fig. 5). However, strain AAP106 has a much lower Chl content per cell than the wild type (Table 2), and the low-temperature fluorescence emission spectrum of strain AAP106 clearly shows that there is less PSI than in the wild type or AAP104 strain (Fig. 4). These observations argue that there are other effects, probably related to altered stability and turnover of PSI and/or to the impact of the changes in transcription, which occur in this strain (Fig. 6; Table S2). The faster recombination of reduced  $[F_A/F_B]^-$  with  $P_{700}^+$  and its inability to be reduced with dithionite indicate that that redox potential of the mixed-ligand [4Fe–4S] cluster in the modified  $F_B$  site is lower than that of the wild type, but this should have no effect on forward electron transfer to flavodoxin. The slower recombination of reduced  $[F_A/F_B]^-$  with  $P_{700}^+$  indicate that that redox potential of the [3Fe–4S] cluster in the modified  $F_B$  site is higher than that of the wild type, a conclusion supported by an earlier redox titration of the [3Fe–4S] cluster in a similar C14A mutant of PsaC (Mehari et al. 1995). Although a more positive midpoint potential would ordinarily disallow reduction of ferredoxin/flavodoxin, this does not necessarily translate to a limitation in electron transfer (Pintscher et al. 2016), as the overall Gibbs free energy change would still be negative, thus allowing for reduction of ferredoxin/flavodoxin ( $E_m' = -420$  mV). While the rate through the [3Fe–4S] cluster would suffer a Boltzmann rate penalty as a consequence of the

uphill electron transfer from the relatively high-potential [3Fe–4S] cluster to flavodoxin, the bottleneck in flavodoxin reduction is probably photon flux, and the rate penalty of this intermediate step would hardly be detectable. Indeed, the presence of [3Fe–4S] clusters as intermediate cofactors in electron transfer chains is not novel (Emptage et al. 1980; Huynh et al. 1980), and the PsaC<sub>C14G</sub> subunit in the PSI complexes in this study draws parallels to the ferredoxin from *A. vinelandii*, which also contains mixed types of Fe/S clusters (Stout 1989) as well as to the medial high-potential [3Fe–4S] cluster in [NiFe] hydrogenase from *Desulfovibrio* species (Rousset et al. 1998). In the latter study, conversion of a high-potential [3Fe–4S] to a low-potential [4Fe–4S] cluster by site-directed mutagenesis (Petrenko and Stein 2015), caused a decrease in midpoint potential of approximately 300 mV with minimal effects on catalytic rate. Thus, it is not unprecedented that a [3Fe–4S] cluster can serve as a cofactor in an electron transfer chain, but to our best knowledge, this is the first reported case of a functional [3Fe–4S] cluster in a Type-1 photosynthetic reaction center.

### Consequence of a long-lifetime terminal electron acceptor

In the PSI complexes of the wild-type strain, electrons mostly reside on the F<sub>A</sub> cluster because the equilibrium constant favors F<sub>A</sub> by about a factor of 10 ( $E_m^{0'} = -580$  mV for F<sub>B</sub> vs.  $-520$  mV for F<sub>A</sub>). The reason for the preferential residence of the electron on the buried F<sub>A</sub> cluster may be to lessen the possibility of electron transfer to dioxygen (Jagannathan et al. 2012; Rutherford et al. 2012). Because the [3Fe–4S] cluster in the F<sub>B</sub>' site has a more positive midpoint potential than the [4Fe–4S] cluster in the F<sub>A</sub> site, and because equilibrium between the two clusters is rapid (Warren et al. 1993; Macedo-Ribeiro et al. 1996), the electron should preferentially reside on F<sub>B</sub> rather than on F<sub>A</sub> in the population of PSI that contains the [3Fe–4S] cluster. This should lead to a greater amount of superoxide radical produced than in the wild type. Indeed, the transcriptional profiling data show a 2.3-fold increase in transcript abundance for *katG* (SYNPCC7002\_A2422), which encodes catalase–peroxidase (Table S2) in strain AAP106. This suggests that cells may be responding to increased production of superoxide anions from dioxygen (Perelman et al. 2003), which could be enhanced if electrons reside on the more exposed F<sub>B</sub> cluster (Jagannathan et al. 2012). On the other hand, the electron should preferentially reside on F<sub>A</sub> rather than on F<sub>B</sub> in the population of PSI that contains the mixed-ligand [4Fe–4S] cluster. Because of this complication, further work is needed to determine whether the

AAP106 cells are more susceptible to damage by molecular oxygen than the wild type.

### Adaptive changes in gene expression in the AAP106 PSI variant

*Synechococcus* 7002 is a robust cyanobacterium that is capable of photoautotrophic growth despite a significant change in the electron transfer chain of PSI. It is possible that the network of adaptive mutations and changes in gene expression throughout the genome in *Synechocystis* 6803 may be less robust and concerted compared to *Synechococcus* 7002, and therefore such changes are unable to rescue or stabilize variant PSI complexes. The global transcriptional analysis suggests numerous changes (spontaneous mutations or regulatory differences) that could help to maintain a Fe/S cluster in the modified F<sub>B</sub> site despite the absence of a coordinating Cys residue (Fig. 6). Principal among these are the increased transcript levels for *suf* operon genes involved in Fe/S cluster biogenesis and regulation (Wang et al. 2004; Jin et al. 2008) (Fig. 6). The higher transcript levels for these genes provide a potential safeguard against photosynthesis-related redox stress (Balasubramanian et al. 2006) in strain AAP106, in which the incorporation of Fe/S clusters into PsaC<sub>C14G</sub> is inferred to occur sub-optimally.

Lowered transcript levels for the *isiAB* operon, as well as for genes encoding two bacterioferritins (Keren et al. 2004), indicate that the cells of strain AAP106 respond transcriptionally as though they are experiencing iron-replete or even iron-excess conditions (Leonhardt and Straus 1993; Duhring et al. 2006) (Table S2), possibly due to the inefficient utilization of iron for Fe/S cluster formation of PSI. Likewise, genes for the synthesis of the siderophore synechobactin were not induced in AAP106, which further indicates that the intracellular iron concentrations were sufficient to keep the Fur repressor in its active state (Ludwig et al. 2015). Collectively, these observations suggest that an enhanced availability of iron that may help strain AAP106 to maintain its Fe/S clusters and lessen iron-induced stress. Additionally, the enhanced production of chaperones including DnaK, GroEL, GroES, GroEL-II (Fig. 6; Table S2) could potentially help to stabilize holo-PsaC with [3Fe–4S] clusters in the F<sub>B</sub> site sufficiently to enhance its assembly into PSI complexes.

It is unclear why a global upregulation in genes of nitrogen metabolism (e.g., *narB*, *nirA*, *nrtP*, *nrtB*, *ntcB*, *amt*, and *glnN*) occurs (Fig. 6; Table S2). A possible explanation is that these genes are upregulated as a response to a decrease in the availability of reduced ferredoxin, which is required for the reduction of nitrate by nitrate reductase (NarB) (Rubio et al. 1996). Nitrogen limitation should have led to a decrease in phycobiliprotein content (Sakamoto and Bryant 1998); however, instead an increase in phycobiliprotein

content was observed in strain AAP106 (Table 2). This observation indicates that nitrogen limitation is not responsible for the enhanced transcription of these genes. An alternative hypothesis is that strain AAP106 produces less proton motive force and has lower ATP levels that affect signaling by GlnB ( $P_{II}$ ) and NtcA. These changes could lead to increased transcription of genes for nitrogen metabolism. The increased phycobiliprotein content can be explained as a means by which cells attempt to partition light energy between PSII and PSI to achieve the proper redox balance between the activities of these two reaction centers.

### Concluding remarks

The goal of this study was to produce PSI complexes *in vivo* containing the PsaC<sub>C14G</sub> variant to build a self-assembling light-driven module similar to the one assembled *in vitro* by Lubner et al. (2011a, b). Future studies will focus on relieving the tight association of PsaC<sub>C14G</sub> in the PSI complex to evaluate steric hindrance as the limiting factor for iron and/or rescue ligand incorporation by knockout mutagenesis of the PsaE and PsaD, the stromal subunit partners of PsaC (Zhao et al. 1990, 1993; Jordan et al. 2001). Additionally, it may still be possible to produce PSI complexes that can be used as the light-driven module of bionanodevices for energy production by cyanobacteria, if strategies such as rescuing  $F_B$  *in vivo* using exogenous dithiolate compounds can be devised to convert the [3Fe–4S] to mixed-ligand [4Fe–4S] clusters. Overall, the findings in this study further expand our knowledge towards building an *in vivo* assembly of a high-throughput bionanodevice that uses a hydrogenase catalyst tethered proximally to PSI by a dithiol-containing molecular wire to enable electron tunneling to the catalytic module.

**Acknowledgements** This study was supported by a grant from the U.S. Department of Energy, Basic Energy Sciences, Division of Materials Sciences and Engineering, under Contract DE-FG02-05ER46222 to J. H. G. and D. A. B. and by NSF grants MCB-1021725 and MCB-1613022 to D. A. B. and J. H. G. We also acknowledge the NSF GK-12 CarbonEARTH grant (award number 0947962) for providing tuition and stipend support to A.A.P. for 3 years and a supplement to NSF grant MCB-1359578 to J.H.G., which provided tuition and stipend support to K.W. for 3 years.

### References

- Anderson ME (1998) Glutathione: an overview of biosynthesis and modulation. *Chem Biol Interact* 111–112:1–14
- Angermayr SA, Hellingwerf KJ, Lindblad P, de Mattos MJT (2009) Energy biotechnology with cyanobacteria. *Curr Opin Biotechnol* 20:257–263
- Antonkine ML, Liu G, Bentrop D, Bryant DA, Bertini I, Luchinat C, Golbeck JH, Stehlik D (2002) Solution structure of the unbound, oxidized Photosystem I subunit PsaC, containing [4Fe–4S] clusters  $F_A$  and  $F_B$ : a conformational change occurs upon binding to Photosystem I. *J Biol Inorg Chem* 7:461–472
- Antonkine ML, Maes EM, Czernuszewicz RS, Breitenstein C, Bill E, Falzone CJ, Balasubramanian R, Lubner C, Bryant DA, Golbeck JH (2007) Chemical rescue of a site-modified ligand to a [4Fe–4S] cluster in PsaC, a bacterial-like dicluster ferredoxin bound to Photosystem I. *Biochim Biophys Acta* 1767:712–724
- Antonkine ML, Koay MS, Boris E, Breitenstein C, Gupta O, Gartner W, Bill E, Lubitz W (2009) Synthesis and characterization of *de novo* designed peptides modeling the binding sites of [4Fe–4S] clusters in photosystem I. *Biochim Biophys Acta* 1787:995–1008
- Asso M, Mbarki O, Guigliarelli B, Yagi T, Bertrand P (1995) EPR and redox characterization of ferredoxins I and II from *Desulfovibrio vulgaris* Miyazaki. *Biochem Biophys Res Commun* 211:198–204
- Balasubramanian R, Shen G, Bryant DA, Golbeck JH (2006) Regulatory roles for IscA and SufA in iron homeostasis and redox stress responses in the cyanobacterium *Synechococcus* sp. strain PCC 7002. *J Bacteriol* 188:3182–3191
- Cameron JC, Pakrasi HB (2010) Essential role of glutathione in acclimation to environmental and redox perturbations in the cyanobacterium *Synechocystis* sp. PCC 6803. *Plant Physiol* 154:1673–1685
- Cantrell A, Bryant DA (1987) Molecular cloning and nucleotide sequence of the *psaA* and *psaB* genes of the cyanobacterium *Synechococcus* sp. PCC 7002. *Plant Mol Biol* 9:453–468
- Davies FK, Work VH, Beliaev AS, Posewitz MC (2014) Engineering limonene and bisabolene production in wild type and a glycogen-deficient mutant of *Synechococcus* sp. PCC 7002. *Front Bioeng Biotechnol* 2:21
- Ducat DC, Way JC, Silver PA (2011) Engineering cyanobacteria to generate high-value products. *Trends Biotechnol* 29:95–103
- Duhring U, Axmann IM, Hess WR, Wilde A (2006) An internal antisense RNA regulates expression of the photosynthesis gene *isiA*. *Proc Natl Acad Sci USA* 103:7054–7058
- Emptage MH, Kent TA, Huynh BH, Rawlings J, Orme-Johnson WH, Munck E (1980) On the nature of the iron-sulfur centers in a ferredoxin from *Azotobacter vinelandii*. Mössbauer studies and cluster displacement experiments. *J Biol Chem* 255:1793–1796
- Fischer N, Setif P, Rochaix JD (1999) Site-directed mutagenesis of the PsaC subunit of photosystem I.  $F_B$  is the cluster interacting with soluble ferredoxin. *J Biol Chem* 274:23333–23340
- Gan F, Zhang S, Rockwell NC, Martin SS, Lagarias JC, Bryant DA (2014) Extensive remodeling of a cyanobacterial photosynthetic apparatus in far-red light. *Science* 345:1312–1317
- Golbeck JH (1995) Resolution and reconstitution of photosystem I. In: Song PS, Horspool WM (eds) *CRC handbook of organic photochemistry and photobiology*. CRC Press, Boca Raton, pp 1407–1419
- Golbeck JH (1999) A comparative analysis of the spin state distribution of *in vivo* and *in vitro* mutants of PsaC. A biochemical argument for the sequence of electron transfer in Photosystem I as  $F_X \rightarrow F_A \rightarrow F_B \rightarrow$  ferredoxin/ferredoxin. *Photosynth Res* 61:107–149
- Golbeck JH, Bryant DA (1991) Photosystem I. *Curr Top Bioenerg* 16:83–177
- Greenbaum E (1985) Platinized chloroplasts: a novel photocatalytic material. *Science* 230:1373–1375
- Grimme RA, Lubner CE, Bryant DA, Golbeck JH (2008) Photosystem I/molecular wire/metal nanoparticle bioconjugates for the photocatalytic production of  $H_2$ . *J Am Chem Soc* 130:6308–6309
- Grimme RA, Lubner CE, Golbeck JH (2009) Maximizing  $H_2$  production in Photosystem I/dithiol molecular wire/platinum nanoparticle bioconjugates. *Dalton Trans* 45:10106–10113
- Hellingwerf KJ, Teixeira de Mattos MJ (2009) Alternative routes to biofuels: light-driven biofuel formation from  $CO_2$  and water based on the ‘photanol’ approach. *J Biotechnol* 142:87–90



- Huynh BH, Moura JJ, Moura I, Kent TA, LeGall J, Xavier AV, Munck E (1980) Evidence for a three-iron center in a ferredoxin from *Desulfovibrio gigas*. Mössbauer and EPR studies. *J Biol Chem* 255:3242–3244
- Iwuchukwu II, Vaughn M, Myers N, O'Neill H, Frymier P, Bruce BD (2010) Self-organized photosynthetic nanoparticle for cell-free hydrogen production. *Nat Nanotechnol* 5:73–79
- Jagannathan B, Shen G, Golbeck JH (2012) The evolution of Type I reaction centers: the response to oxygen. In: Burnap R, Vermaas W (eds) *Functional genomics and evolution of photosynthetic systems, advances photosynthesis and respiration*, vol 33. Springer, Dordrecht, pp 285–316
- Jin Z, Heinnickel M, Krebs C, Shen G, Golbeck JH, Bryant DA (2008) Biogenesis of iron-sulfur clusters in photosystem I: holo-NfuA from the cyanobacterium *Synechococcus* sp. PCC 7002 rapidly and efficiently transfers [4Fe-4S] clusters to apo-PsaC in vitro. *J Biol Chem* 283:28426–28435
- Johnson MK, Bennett DE, Fee JA, Sweeney WV (1987) Spectroscopic studies of the seven-iron-containing ferredoxins from *Azotobacter vinelandii* and *Thermus thermophilus*. *Biochim Biophys Acta* 911:81–94
- Jordan P, Fromme P, Witt HT, Klukas O, Saenger W, Krauss N (2001) Three-dimensional structure of cyanobacterial photosystem I at 2.5 Å resolution. *Nature* 411:909–917
- Jung Y-S, Yu L, Golbeck JH (1995) Reconstitution of iron-sulfur center F<sub>B</sub> results in complete restoration of NADP<sup>+</sup> photoreduction in Hg-treated Photosystem I complexes from *Synechococcus* sp. PCC 6301. *Photosynth Res* 46:249–255
- Jung Y-S, Vassiliev IR, Qiao F, Yang F, Bryant DA, Golbeck JH (1996) Modified ligands to F<sub>A</sub> and F<sub>B</sub> in photosystem I. III. Proposed chemical rescue of a [4Fe-4S] cluster with an external thiolate in alanine, glycine, and serine mutants of PsaC. *J Biol Chem* 271:31135–31144
- Jung Y-S, Vassiliev IR, Yu J, McIntosh L, Golbeck JH (1997) Strains of *Synechocystis* sp. PCC 6803 with altered PsaC. II. EPR and optical spectroscopic properties of F<sub>A</sub> and F<sub>B</sub> in aspartate, serine, and alanine replacements of cysteines 14 and 51. *J Biol Chem* 272:8040–8049
- Keren N, Aurora R, Pakrasi HB (2004) Critical roles of bacterioferritins in iron storage and proliferation of cyanobacteria. *Plant Physiol* 135:1666–1673
- Leonhardt K, Straus NA (1993) Photosystem II genes *isiA*, *psbDI* and *psbC* in *Anabaena* sp. PCC 7120: cloning, sequencing and the transcriptional regulation in iron-stressed and iron-replete cells. *Plant Mol Biol* 24:63–73
- Lubner CE, Grimme R, Bryant DA, Golbeck JH (2010) Wiring photosystem I for direct solar hydrogen production. *Biochemistry* 49:404–414
- Lubner CE, Applegate AM, Knorzer P, Ganago A, Bryant DA, Happe T, Golbeck JH (2011a) Solar hydrogen-producing bionanodevice outperforms natural photosynthesis. *Proc Natl Acad Sci USA* 108:20988–20991
- Lubner C, Bryant DA, Golbeck JH (2011b) Wired reaction centers. In: Hillier W, Wydrzynski T (eds) *Molecular solar fuels*. Royal Society of Chemistry, London, pp 464–505
- Ludwig M, Bryant DA (2011) Transcription profiling of the model cyanobacterium *Synechococcus* sp. strain PCC 7002 by Next-Gen (SOLiD™) sequencing of cDNA. *Front Microbiol* 2:41
- Ludwig M, Bryant DA (2012) Acclimation of the global transcriptome of the cyanobacterium *Synechococcus* sp. strain PCC 7002 to nutrient limitations and different nitrogen sources. *Front Microbiol* 3:145
- Ludwig M, Chua T-T, Chew C-Y, Bryant DA (2015) Fur-type transcriptional repressors and metal homeostasis in the cyanobacterium *Synechococcus* sp. PCC 7002. *Front Microbiol* 6:1217
- Macedo-Ribeiro S, Darimont B, Sterner R, Huber R (1996) Small structural changes account for the high thermostability of 1[4Fe-4S] ferredoxin from the hyperthermophilic bacterium *Thermotoga maritima*. *Structure* 4:1291–1301
- Machado IM, Atsumi S (2012) Cyanobacterial biofuel production. *J Biotechnol* 162:50–56
- Malkin R, Bearden AJ (1971) Primary reactions of photosynthesis: photoreduction of a bound chloroplast ferredoxin at low temperature as detected by EPR spectroscopy. *Proc Natl Acad Sci USA* 68:16–19
- Mehari T, Qiao F, Scott MP, Nellis DF, Zhao J, Bryant DA, Golbeck JH (1995) Modified ligands to F<sub>A</sub> and F<sub>B</sub> in photosystem I. I. Structural constraints for the formation of iron-sulfur clusters in free and rebound PsaC. *J Biol Chem* 270:28108–28117
- Nozzi NE, Oliver JWK, Atsumi S (2013) Cyanobacteria as a platform for biofuel production. *Front Bioeng Biotechnol* 1:7
- Perelman A, Uzan A, Hacoheh D, Schwarz R (2003) Oxidative stress in *Synechococcus* sp. strain PCC 7942: various mechanisms for H<sub>2</sub>O<sub>2</sub> detoxification with different physiological roles. *J Bacteriol* 185:3654–3660
- Pérez AA (2016) Expanding the biotechnological potential of the model cyanobacterium *Synechococcus* sp. strain PCC 7002. Ph. D. Dissertation, The Pennsylvania State University
- Pérez AA, Liu Z, Rodionov DA, Li Z, Bryant DA (2016a) Complementation of cobalamin auxotrophy in *Synechococcus* sp. strain PCC 7002 and validation of a putative cobalamin riboswitch in vivo. *J Bacteriol* 198:2743–2752
- Pérez AA, Rodionov DA, Bryant DA (2016b) Identification and regulation of genes for cobalamin transport in the cyanobacterium *Synechococcus* sp. strain PCC 7002. *J Bacteriol* 198:2753–2761
- Petrenko A, Stein M (2015) Rates and routes of electron transfer of [NiFe]-hydrogenase in an enzymatic fuel cell. *J Phys Chem B* 119:13870–13882
- Pintscher S, Kuleta P, Cieluch E, Borek A, Sarewicz M, Osyczka A (2016) Tuning of hemes *b* equilibrium redox potential is not required for cross-membrane electron transfer. *J Biol Chem* 291:6872–6881
- Rippka R, Deruelles J, Waterbury JB, Herdman M, Stanier RY (1979) Generic assignments, strain histories and properties of pure cultures of cyanobacteria. *J Gen Microbiol* 278:1–61
- Roche B, Aussel L, Ezraty B, Mandin P, Py B, Barras F (2013) Iron/sulfur proteins biogenesis in prokaryotes: formation, regulation and diversity. *Biochim Biophys Acta* 1827:455–469
- Rousset M, Montet Y, Guigliarelli B, Forget N, Asso M, Bertrand P, Fontecilla-Camps JC, Hatchikian EC (1998) [3Fe-4S] to [4Fe-4S] cluster conversion in *Desulfovibrio fructosovorans* [NiFe] hydrogenase by site-directed mutagenesis. *Proc Natl Acad Sci USA* 95:11625–11630
- Rubio LM, Herrero A, Flores E (1996) A cyanobacterial *narB* gene encodes a ferredoxin-dependent nitrate reductase. *Plant Mol Biol* 30:845–850
- Rupprecht J, Hankamer B, Mussgnug JH, Ananyev G, Dismukes C, Kruse O (2006) Perspectives and advances of biological H<sub>2</sub> production in microorganisms. *Appl Microbiol Biotechnol* 72:442–449
- Rutherford AW, Osyczka A, Rappaport F (2012) Back-reactions, short-circuits, leaks and other energy wasteful reactions in biological electron transfer: Redox tuning to survive life in O<sub>2</sub>. *FEBS Lett* 586:603–616
- Sakamoto T, Bryant DA (1998) Growth at low temperature causes nitrogen limitation in the cyanobacterium *Synechococcus* sp. PCC 7002. *Arch Microbiol* 169:10–19
- Sauer K, Mathis P, Acker S, van Best JA (1978) Electron acceptors associated with P-700 in Triton solubilized photosystem I particles from spinach chloroplasts. *Biochim Biophys Acta* 503:120–134

- Savakis P, Hellingwerf KJ (2015) Engineering cyanobacteria for direct biofuel production from CO<sub>2</sub>. *Curr Opin Biotechnol* 33:8–14
- Schluchter WM, Shen G, Zhao J, Bryant DA (1996) Characterization of *psaI* and *psaL* mutants of *Synechococcus* sp. strain PCC 7002: a new model for state transitions in cyanobacteria. *Photochem Photobiol* 64:53–66
- Shen G, Bryant DA (1995) Characterization of a *Synechococcus* sp. strain PCC 7002 mutant lacking photosystem I. Protein assembly and energy distribution in the absence of the Photosystem I reaction center core complex. *Photosynth Res* 44:41–53
- Shen G, Antonkine ML, van der Est A, Vassiliev IR, Brettel K, Bittl R, Zech SG, Zhao J, Stehlik D, Bryant DA, Golbeck JH (2002a) Assembly of photosystem I. II. Rubredoxin is required for the in vivo assembly of F<sub>X</sub> in *Synechococcus* sp. PCC 7002 as shown by optical and EPR spectroscopy. *J Biol Chem* 277:20355–20366
- Shen G, Zhao J, Reimer SK, Antonkine ML, Cai Q, Weiland SM, Golbeck JH, Bryant DA (2002b) Assembly of photosystem I. I. Inactivation of the *rubA* gene encoding a membrane-associated rubredoxin in the cyanobacterium *Synechococcus* sp. PCC 7002 causes a loss of photosystem I activity. *J Biol Chem* 277:20343–20354
- Shen G, Balasubramanian R, Wang T, Wu Y, Hoffart LM, Krebs C, Bryant DA, Golbeck JH (2007) SufR coordinates two [4Fe-4S]<sup>2+,1+</sup> clusters and functions as a transcriptional repressor of the *sufB-CDS* operon and an autoregulator of *sufR* in cyanobacteria. *J Biol Chem* 282:31909–31919
- Shinkarev VP, Zybailov B, Vassiliev IR, Golbeck JH (2002) Modeling of the P700<sup>+</sup> charge recombination kinetics with phyloquinone and plastoquinone-9 in the A<sub>1</sub> site of Photosystem I. *Biophys J* 83:2885–2897
- Silver SC, Niklas J, Du P, Poluektov OG, Tiede DM, Utschig LM (2013) Protein delivery of a Ni catalyst to photosystem I for light-driven hydrogen production. *J Am Chem Soc* 135:13246–13249
- Stevens SE, Porter RD (1980) Transformation in *Agmenellum quadruplicatum*. *Proc Natl Acad Sci USA* 77:6052–6056
- Stout CD (1989) Refinement of the 7 Fe ferredoxin from *Azotobacter vinelandii* at 1.9 Å resolution. *J Mol Biol* 205:545–555
- Suzuki JY, Bauer CE (1992) Light-independent chlorophyll biosynthesis: involvement of the chloroplast gene *chlL* (*frxC*). *Plant Cell* 4:929–940
- Utschig LM, Dimitrijevic NM, Poluektov OG, Chemerisov KL, Mulfort KL, Tiede DM (2011) Photocatalytic hydrogen production from noncovalent biohybrid photosystem I/Pt nanoparticle complexes. *J Phys Chem Lett* 2:236–241
- Utschig LM, Soltau SR, Tiede DM (2015) Light-driven hydrogen production from photosystem I-catalyst hybrids. *Curr Opin Chem Biol* 25:1–8
- van der Est A (2001) Light-induced spin polarization in Type I photosynthetic reaction centers. *Biochim Biophys Acta* 1507:212–225
- Vassiliev IR, Jung Y-S, Mamedov MD, Semenov A, Golbeck JH (1997) Near-IR absorbance changes and electrogenic reactions in the microsecond-to-second time domain in Photosystem I. *Biophys J* 72:301–315
- Vassiliev IR, Antonkine ML, Golbeck JH (2001) Iron-sulfur clusters in type I reaction centers. *Biochim Biophys Acta* 1507:139–160
- Wang T, Shen G, Balasubramanian R, McIntosh L, Bryant DA, Golbeck JH (2004) The *sufR* gene (sl10088 in *Synechocystis* sp. strain PCC 6803) functions as a repressor of the *sufBCDS* operon in iron-sulfur cluster biogenesis in cyanobacteria. *J Bacteriol* 186:956–967
- Warren PV, Smart LB, McIntosh L, Golbeck JH (1993) Site-directed conversion of cysteine-565 to serine in PsaB of photosystem I results in the assembly of [3Fe-4S] and [4Fe-4S] clusters in F<sub>X</sub>. A mixed-ligand [4Fe-4S] cluster is capable of electron transfer to F<sub>A</sub> and F<sub>B</sub>. *Biochemistry* 32:4411–4419
- Xu Q, Jung Y-S, Chitnis VP, Guikema JA, Golbeck JH, Chitnis PR (1994) Mutational analysis of photosystem I polypeptides in *Synechocystis* sp. PCC 6803. Subunit requirements for reduction of NADP<sup>+</sup> mediated by ferredoxin and flavodoxin. *J Biol Chem* 269:21512–21518
- Xu Y, Alvey RM, Byrne PO, Graham JE, Shen G, Bryant DA (2011) Expression of genes in cyanobacteria: adaptation of endogenous plasmids as platforms for high-level gene expression in *Synechococcus* sp. PCC 7002. *Methods Mol Biol* 684:273–293
- Yu L, Zhao J, Lu W, Bryant DA, Golbeck JH (1993) Characterization of the [3Fe-4S] and [4Fe-4S] clusters in unbound PsaC mutants C14D and C51D. Midpoint potentials of the single [4Fe-4S] clusters are identical to F<sub>A</sub> and F<sub>B</sub> in bound PsaC of photosystem I. *Biochemistry* 32:8251–8258
- Yu J, Smart LB, Jung Y-S, Golbeck JH, McIntosh L (1995a) Absence of PsaC subunit allows assembly of photosystem I core but prevents the binding of PsaD and PsaE in *Synechocystis* sp. PCC 6803. *Plant Mol Biol* 29:311–342
- Yu L, Vassiliev IR, Jung Y-S, Bryant DA, Golbeck JH (1995b) Modified ligands to F<sub>A</sub> and F<sub>B</sub> in Photosystem I. II. Characterization of a mixed ligand [4Fe-4S] cluster in the C51D mutant of PsaC upon rebinding to P700-F<sub>X</sub> cores. *J Biol Chem* 270:28118–28125
- Yu L, Bryant DA, Golbeck JH (1995c) Evidence for a mixed-ligand [4Fe-4S] cluster in the C14D mutant of PsaC. Altered reduction potentials and EPR spectral properties of the F<sub>A</sub> and F<sub>B</sub> clusters on rebinding to the P700-F<sub>X</sub> core. *Biochemistry* 34:7861–7868
- Yu J, Vassiliev IR, Jung Y-S, Golbeck JH, McIntosh L (1997) Strains of *Synechocystis* sp. PCC 6803 with altered PsaC. I. Mutations incorporated in the cysteine ligands of the two [4Fe-4S] clusters F<sub>A</sub> and F<sub>B</sub> of photosystem I. *J Biol Chem* 272:8032–8039
- Yu J, Shen G, Wang T, Bryant DA, Golbeck JH, McIntosh L (2003) Suppressor mutations in the study of photosystem I biogenesis: sl10088 is a previously unidentified gene involved in reaction center accumulation in *Synechocystis* sp. strain PCC 6803. *J Bacteriol* 185:3878–3887
- Zhang S, Shen G, Li Z, Golbeck JH, Bryant DA (2014) Vipp1 is essential for the biogenesis of photosystem I but not thylakoid membranes in *Synechococcus* sp. PCC 7002. *J Biol Chem* 289:15904–15914
- Zhang S, Liu Y, Bryant DA (2015) Metabolic engineering of *Synechococcus* sp. PCC 7002 to produce poly-3-hydroxybutyrate and poly-3-hydroxybutyrate-co-4-hydroxybutyrate. *Metab Eng* 32:174–183
- Zhao J, Warren PV, Li N, Bryant DA, Golbeck JH (1990) Reconstitution of electron transport in photosystem I with PsaC and PsaD proteins expressed in *Escherichia coli*. *FEBS Lett* 276:175–180
- Zhao J, Li N, Warren PV, Golbeck JH, Bryant DA (1992) Site-directed conversion of a cysteine to aspartate leads to the assembly of a [3Fe-4S] cluster in PsaC of photosystem I. The photoreduction of F<sub>A</sub> is independent of F<sub>B</sub>. *Biochemistry* 31:5093–5099
- Zhao J, Snyder WB, Muhlenhoff U, Rhiel E, Warren PV, Golbeck JH, Bryant DA (1993) Cloning and characterization of the *psaE* gene of the cyanobacterium *Synechococcus* sp. PCC 7002: characterization of a *psaE* mutant and overproduction of the protein in *Escherichia coli*. *Mol Microbiol* 9:183–194
- Zhao J, Li R, Bryant DA (1998) Measurement of photosystem I activity with photoreduction of recombinant flavodoxin. *Anal Biochem* 264:263–270
- Zhou J, Zhang H, Meng H, Zhu Y, Bao G, Zhang Y, Li Y, Ma Y (2014) Discovery of a super-strong promoter enables efficient production of heterologous proteins in cyanobacteria. *Sci Rep* 4:4500